

CRYO-ELECTRONIC & NOISE



DÉTECTION DE RAYONNEMENT
À TRÈS BASSE TEMPÉRATURE

Damien PRÉLE - APC
DRTBT2024 - Mars 2024
<https://drtbt.neel.cnrs.fr>

Ultra sensitive cryogenic detectors

- ▶ **Bolometers** / Calorimeters
- ▶ **Josephson** junction based detectors like SQUID (Superconducting QUantum Interference Device) and STJ (Superconducting Tunnel Junctions)
- ▶ **KID** (Kinetic Inductance Detector)
- ▶ **SNSPD** (Superconducting Nanowire Single-Photon Detector)
- ▶ ...

Front-end cryogenic **readout** requirement

Basic function of a front-end readout → **AMPLIFICATION**

CRYOGENIC environment allows to achieve extremely low noise performances

⇒ **NOISE** of the cryogenic readout chain is an essential point

Anyway, Cryogenic T is not a "magic" solution to reduce noise

Amplification = increase in amplitude

- ▶ **Power: active devices are required for power applications**
- ▶ **Voltage or Current:** Current or voltage amplification can be done at equal power using transformers or resonant circuit



- ☞ A *buffer* (common emitter) voltage gain = 1, provides a current gain (high Z_{in} and low Z_{out}) leading to power gain $G_P = G_U G_I$ avec $G_U \rightarrow$ and $G_I \nearrow$
- ☞ A opamp ($Z_{out} \approx 50\Omega$) amplifying a voltage signal of a 50Ω source, provides also a power gain
- ☞ A MOS with an isolated grid, provides a power gain $\rightarrow \infty!$

SNR degradation & readout detection chain

⇒ **The Front End amplifier stage** of a tiny signal is at the same times :

- ▶ The require function to prevent **noise/parasite contaminations**,
- ▶ The **main source of noise** of the readout chain.

It is important to amplify as early as possible in detection chain and avoid any signal attenuation. Once amplified, the amplitude of the signal becomes large compared to the amplitude of the following stages noise.

Thermal noise

Identify by John Bertrand Johnson in 1926

thermal agitation of the charge carriers inside an electrical conductor

50

NATURE

[JANUARY 8, 1927

Thermal Agitation of Electricity in Conductors.

ORDINARY electric conductors are sources of spontaneous fluctuations of voltage which can be measured with sufficiently sensitive instruments. This property of conductors appears to be the result of thermal agitation of the electric charges in the material of the conductor.

The effect has been observed and measured for various conductors, in the form of resistance units, by means of a vacuum tube amplifier terminated in a thermocouple. It manifests itself as a part of the phenomenon which is commonly called 'tube noise.' The part of the effect originating in the resistance gives rise to a mean square voltage fluctuation V^2 which is proportional to the value R of that resistance. The ratio V^2/R is independent of the nature, or shape of the conductor, being the same for resistances of metal wire, graphite, thin metallic films, films of drawing ink, and strong or weak electrolytes. It does, however, depend on temperature and is proportional to the absolute temperature of the resistance. This dependence on temperature demonstrates that the component of the noise which is proportional to R comes from the conductor and not from the vacuum tube.

No. 2984, VOL. 119]

A similar phenomenon appears to have been observed and correctly interpreted in connexion with a *current sensitive* instrument, the string galvanometer (W. Einthoven, W. F. Einthoven, W. van der Horst, and H. Hirschfeld, *Physica*, 5, 358-360, No. 11/12, 1925). What is being measured in these cases is the effect upon the measuring device of continual shock excitation resulting from the random interchange of thermal energy and energy of electric potential or current in the conductor. Since the effect is the same for different conductors, it is evidently not dependent on the specific mechanism of conduction.

The amount and character of the observed noise depend upon the frequency-characteristic of the amplifier, as would be expected from experience with the small-shot effect. The apparent input power originating in the resistance is of the order 10^{-18} watt at room temperature. The corresponding output power is proportional to the area under the graph of *power amplification—frequency*, at least in the range of audio frequencies. The magnitude of the 'initial noise,' when the quietest tubes are used without input resistance, is about the same as that produced by a resistance of 5000 ohms at room temperature in the input circuit. For the technique of amplification, therefore, the effect means that the limit to the smallness of voltage which can be usefully amplified is often set, not by the vacuum tube, but by the very matter of which electrical circuits are built.

J. B. JOHNSON.

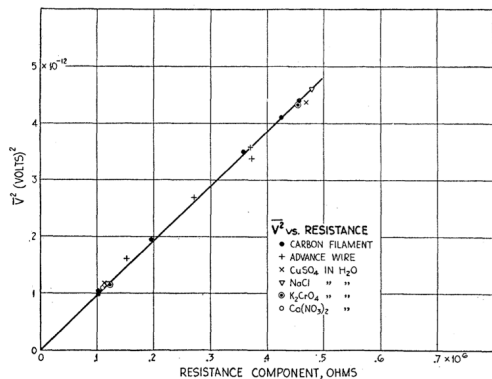
Bell Telephone Laboratories, Inc.,
New York, N.Y., Nov. 17.

Thermal noise

Measured by John B. Johnson in 1926

$$\text{Voltage noise} \propto \sqrt{R}$$

independant of the nature of the resistance



Thermal Agitation of Electricity J. B. Johnson, PHYSICAL REVIEW, July, 1928

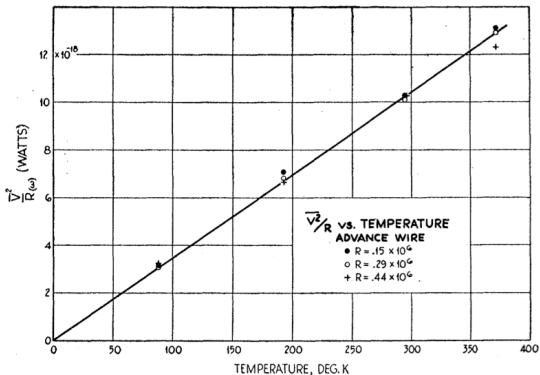
John Bertrand Johnson
(1887-1970)

Thermal noise

Measured by John B. Johnson in 1926

DSP \propto à T

Independently to the R value



John Bertrand Johnson
(1887-1970)

Thermal Agitation of Electricity J. B. Johnson, PHYSICAL REVIEW, July, 1928

Thermal noise

Interpreted by Harry Nyquist in 1928

JULY, 1928

PHYSICAL REVIEW

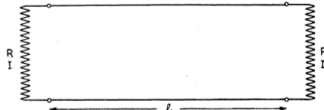
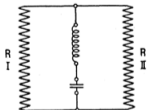
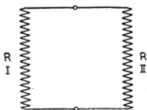
VOLUME 32

THERMAL AGITATION OF ELECTRIC CHARGE IN CONDUCTORS*

By H. NYQUIST

ABSTRACT

The electromotive force due to thermal agitation in conductors is calculated by means of principles in thermodynamics and statistical mechanics.



$$E_v^2 d\nu = 4R_v kT d\nu$$

$$E_v^2 d\nu = 4R_v h d\nu / (e^{h\nu/kT} - 1)$$

Quantum limitation (@ high f and/or very low T)

Generalization including a quantum approach (similar to black body radiation) :

Electric energy \rightarrow multiply by hf DSP thermal noise :

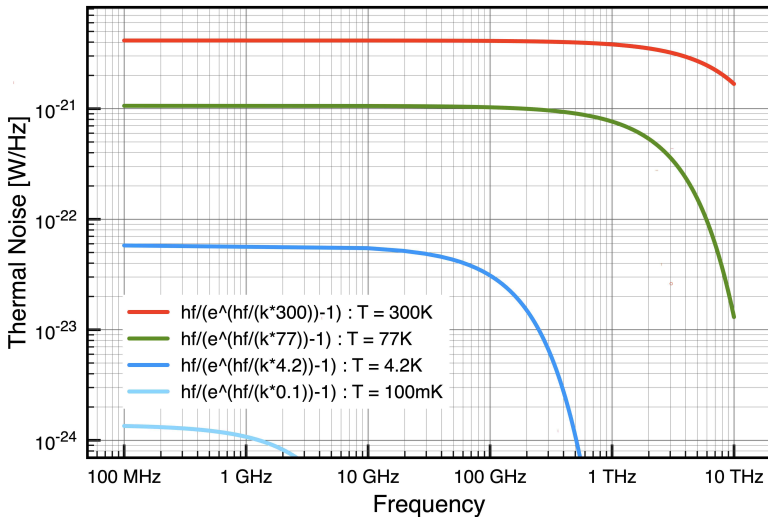
$$S = \frac{hf}{e^{\frac{hf}{k_B T}} - 1}$$

$$= \frac{hf}{\frac{hf}{k_B T} + \frac{1}{2!} \left(\frac{hf}{k_B T}\right)^2 + \frac{1}{3!} \left(\frac{hf}{k_B T}\right)^3 + \dots}$$

$$\approx k_B T \quad \text{only if } k_B T \gg hf$$

- ☞ @ 300 K white up to 6 THz
- ☞ @ 300 mK "only" up to 6 GHz !

DSP de bruit thermique d'une resistance : $S = \frac{hf}{e^{\frac{hf}{k_B T}} - 1}$



Johnson noise cut off take in consideration for Johnson thermometry

At the very lowest temperatures, Nyquist's law may not be a sufficient approximation of the fluctuation dissipation relation (1). The relative error in Nyquist's law is given by the series expansion of the Planck factor (see (2))

$$\frac{(hf / kT)}{\exp(hf / kT) - 1} = 1 - \frac{hf}{2kT} + \dots \approx 1 - 2.4 \times 10^{-11} \frac{f}{T}, \quad (23)$$

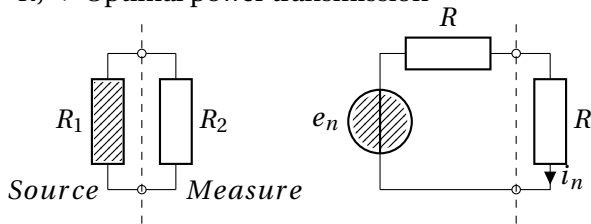
so that a JNT using Nyquist's law at temperatures near 1 mK and with an average operating frequency of 100 kHz is accurate to about 0.24%.

J. F. Qu et al. Johnson Noise Thermometry

Available/Measurable thermal noise power

$k_B T \Delta f \rightarrow$ Puissance maximale disponible

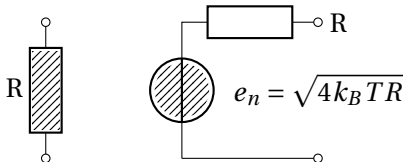
To measure $P = k_B T \Delta f$, a matching impedance is required
($R_1 = R_2 = R$) \rightarrow Optimal power transmission



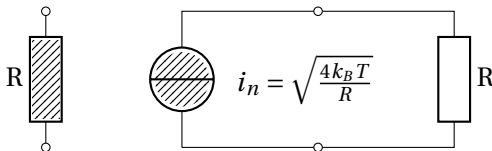
$$k_B T \Delta f = R i_n^2 = R \left(\frac{e_n}{2R} \right)^2 = \frac{e_n^2}{4R} \rightarrow e_n^2 = 4k_B T R |_{\Delta f=1\text{Hz}}$$

Voltage and Current noise spectral density

$$e_n = \sqrt{4k_B T R} \text{ [V}/\sqrt{\text{Hz}}]$$



$$i_n = \sqrt{\frac{4k_B T}{R}} \text{ [A}/\sqrt{\text{Hz}}]$$



Equivalent noise resistance and noise temperature

Assuming a white noise spectral density S_v and S_i ; and a "source/detector" impedance R_s we modeled as a :

- ▶ **Noise equivalent resistance:** Resistance producing the same Johnson noise than the S_v and S_i contribution (define at which temperature).

$$R_{eq} = \frac{S_v + R_s^2 S_i}{4k_B T_0}$$

- ▶ **Noise equivalent temperature :** at which temperature a R_0 (often $R_0 = R_s = 50\Omega$) produces the same noise as the S_v and S_i contributions

$$T_{eq} = \frac{S_v + R_s^2 S_i}{4k_B R_0}$$

Noise in electronic devices

Johnson noise = Real resistances

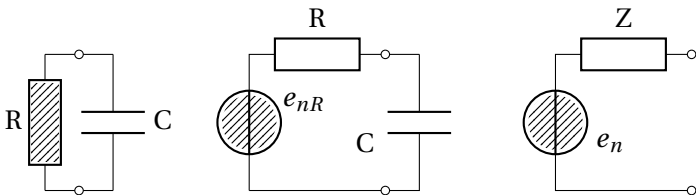
- ✓ The Johnson noise is only associated to the \Re impedance
- ✗ Imaginary parts (L or C) and Dynamic impedances or active charges (h_{11} , $1/g_m$, $R_{DS} \dots$) → do not produces Johnson noise
(except maybe the MOS channel noise in Strong inversion $\frac{2}{3}4k_B T g_m$ where the resistance of the channel is real)

☞ But sometimes people misuse the term by referring to ...

- ▶ "Capacitive" noise $\frac{k_B T}{C}$
- ▶ "Thermal noise of a bipolar transistor" $\frac{4k_B T}{2g_m}$

Voltage noise $k_B T / C$ (noise integrated $f[0 \rightarrow \infty]$)

integrated noise of a resistor filtered by a capacitor



$$Z = R // C = \frac{R}{\sqrt{1 + \left(\frac{f}{f_c}\right)^2}} \quad \text{avec } f_c = \frac{1}{2\pi RC} \rightarrow \Delta f = \frac{\pi}{2} f_c = \frac{1}{4RC}$$

$$e_n^2 = \frac{e_{nR}^2}{1 + \left(\frac{f}{f_c}\right)^2} \rightarrow v_{eff} = e_{nR} \times \sqrt{\Delta f} = \sqrt{4k_B T R \frac{1}{4RC}} = \sqrt{\frac{k_B T}{C}}$$

$$v_{eff}^2 = \frac{k_B T}{C} \quad \forall R!$$

⇒ but T is the resistor temperature

Charge noise $k_B T C$

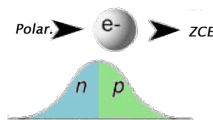
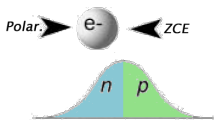
$$Q = CV$$

$$v_{eff} = \sqrt{\frac{k_B T}{C}} \rightarrow Q_n = \sqrt{k_B T C}$$

Charge and voltage noise in capacitors

C	$\frac{\sqrt{k_B T C}}{q}$	$\sqrt{k_B T / C}$
1 μ F	400000 e^-	64 nV
1 nF	13000 e^-	2 μ V
1 pF	400 e^-	64 μ V
1 fF	13 e^-	2 mV
1 aF	0,4 e^-	64 mV

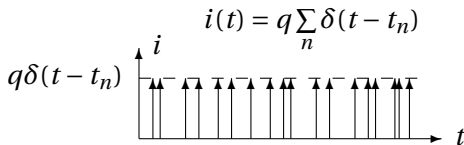
discrete nature of electric charge ; visible in the fast transit of e^- in a potential depleted zone / junction (Poisson distribution)



Op Aspa for everyone - TI

a "Shot !" occurs every electron passing through the junction depleted zone

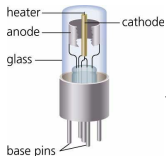
Current = discrete transfert of charges q at arbitrary time t_n



Shot noise in a junction

- ▶ Shot noise → fast transit
- ▶ Time correlation crossing the device
 - ▶ neglectable recombinations (nb e^- emitted = received)
 - ▶ neglectable lattice interaction / delay, large relaxation times (average time between "collisions") τ_r

Transit time crossing the depleted zone τ_t :



$$\tau_t \ll \tau_r$$

shot noise discovered in vacuum tube by
Walter Schottky in 1918



"Schottky expression"

Current spectral density [A^2/Hz]

$$S_i = 2qI$$

with I the DC current crossing the junction

White noise $\forall f$ and T

RMS noise over 1 Hz

$$i_{eff|\Delta f=1Hz} = \sqrt{S_i} = \sqrt{2qI}$$

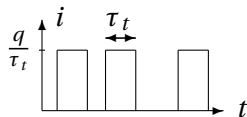
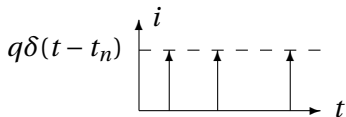
N.A.: assuming a diode bias with $I = 1 \text{ mA}$:

$$\sqrt{S_i} = \sqrt{2 \times 1.6 \cdot 10^{-19} \times 10^{-3}} = 18 \text{ pA}/\sqrt{Hz}$$

$q \approx 1,6 \times 10^{-19} \text{ [C]}$ ou [A.s] est la valeur absolue de la charge de l' e^-

Shot noise in high frequency

Transit time e^- through a junction τ_t

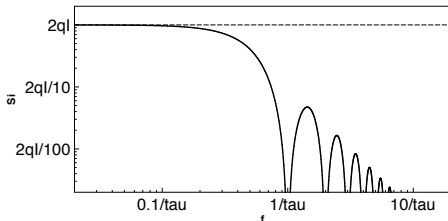


Shot noise spectral density in HF

$$S_i = 2qI \left[\frac{\sin(\pi f \tau)}{\pi f \tau} \right]^2$$

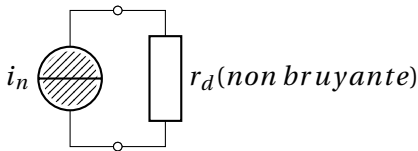
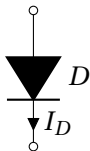
A.N. $\tau_t = 10 \text{ ps}$:

$$\frac{1}{\tau} = 100 \text{ GHz}!$$



Small signal noise model

diode equivalent noise small signal schematic



$$r_d = \frac{k_B T}{q I_D}$$

$$S_i = 2q I_D$$

voltage noise $S_i = 2q I_D \left(\frac{k_B T}{q I_D} \right)^2 = 2 \frac{(k_B T)^2}{q I_D} \dots 4k_B T \frac{r_d}{2}$

⇒ finally, shot noise is depending on temperature ... but it is not means that it is a Johnson noise !

Non-Fondamental noise

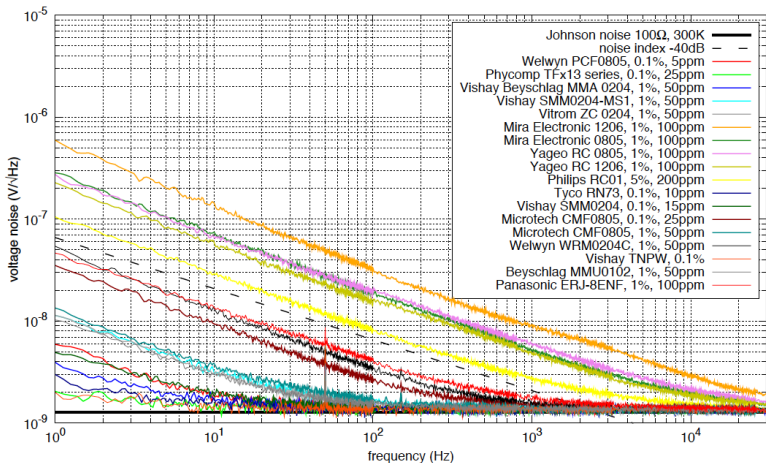
Excess noises \neq Johnson & Shot)

Non/Less predictable noise, not well understood

Shot noise may be include in excess noise, because it disappear with no bias

- ▶ *Avalanche* -> M factor on the shot noise
- ▶ *Generation - recombinaison* (GR ou *burst noise*)
 - ▶ *Telegraphic noise*
 - ▶ $1/f$ (Flicker noise)

Noise in commercial SMD with current



Noise of surface-mount devices (SMD) with 100Ω up to a max. power dissipation of 1 W (U=10V)

"Resistor Current Noise Measurements" - Frank Seifert

Low frequency noise \longrightarrow traps

The low frequency noise is associated to **traps**

Generation recombinaison

Arbitrary number of carriers under electric field:

\nearrow generation :

e^- trap \longrightarrow bande de conduction

trou trap \longrightarrow bande de valence

\searrow recombinaisons :

e^- bande de conduction \longrightarrow trap

trou bande de valence \longrightarrow trap

Generation- recombinations - *GR noise*

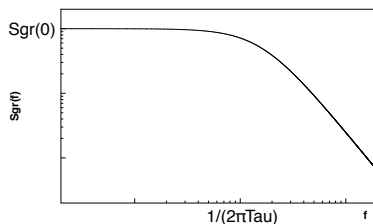
drift current fluctuation

Arbitrary rate of generation recombinations in traps (defects, doping, stats of surface)

Trap relaxations (carrier life time) $\tau_r \ll \tau_t$

$$S_{GR} \propto \frac{I^2 \tau_r}{1 + (2\pi f \tau_r)^2}$$

Lorentzian spectrum $\leftarrow TF(I^2 e^{-t/\tau})$



Generation-recombinations \rightarrow A single G-R process dominates
 τ_r characteristics of an exponential "relaxation"

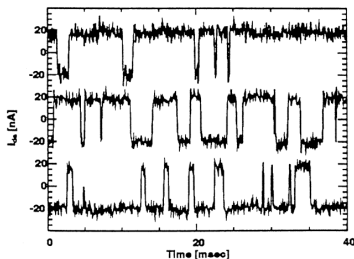
Different relaxation times superposition

multiple generations - recombinaison process

Telegraphic noise

2 levels system or more: multiple time constants τ_r

$$S_{2level} \propto \frac{4(\Delta I)^2}{(\tau_1 + \tau_2) \left[\left(\frac{1}{\tau_1} + \frac{1}{\tau_2} \right)^2 + (2\pi f)^2 \right]}$$



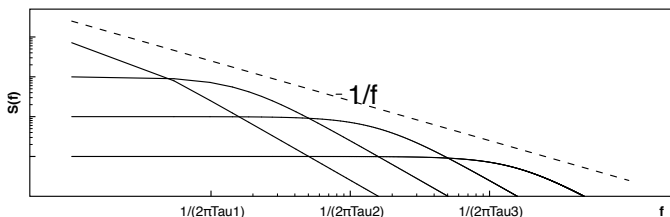
1/f - flicker noise

Large number of generations-recombinaisons processes

→ large number of time constants τ_i

Flicker noise

- ▶ Large number of G-R: e^- number fluctuation ; due to defect, ion and any traps (recombinaison center - present in surface)
→ Large number of Lorentzian spectrums ($\neq f_c$)



$$\begin{aligned}
 S &\propto I^2 \sum_i \frac{\tau_i}{1+(2\pi f\tau_i)^2} = I^2 \int_{\tau_{min}}^{\tau_{max}} \frac{\tau_i}{1+(2\pi f\tau_i)^2} \\
 &= \frac{I^2}{2\pi f} [\arctan(2\pi f\tau_{max}) - \arctan(2\pi f\tau_{min})] \approx \frac{I^2}{4f}
 \end{aligned}$$

- ▶ Mobility fluctuation leads also to: "volume" noise

Low frequency noise bellow 0.1 Hz ... and thermal drift

$f < 10^{-2} Hz \rightarrow$ Thermal fluctuations

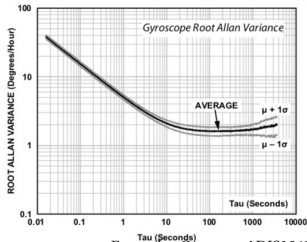
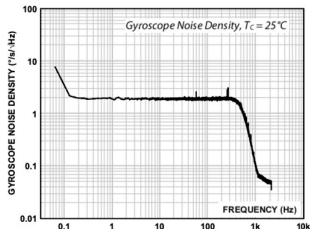
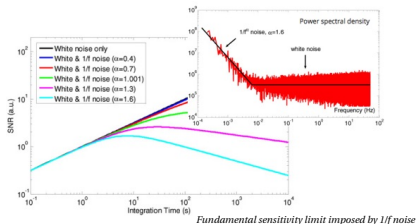
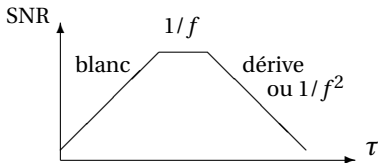
Measured noise down to about $10^{-5} Hz \equiv 1$ day :

- ▶ The drifts are indistinguishable from the low frequency noise
- ▶ The Johnson noise is not anymore white ... because T is not anymore a constante

Allan variance

↗ integration times τ

≠ ↗ SNR



Example : Gyroscop ADIS16490

Empirical modelization of the 1/f noise

frequency dependance

$$S_i \propto \frac{1}{f^\gamma} \quad \text{typical values : } 0.8 < \gamma < 1.3$$

current dependancies

$$S_i \propto I^\alpha \quad \text{typical values : } 0.5 < \alpha < 2$$

current density dependancies $\alpha = 1$

$$S_i \propto \frac{I^\alpha}{A} \quad A = \text{surface presented to the current}$$

Empirical parameter K

$$S_i = \frac{K}{A} \times \frac{I^\alpha}{f^\gamma}$$

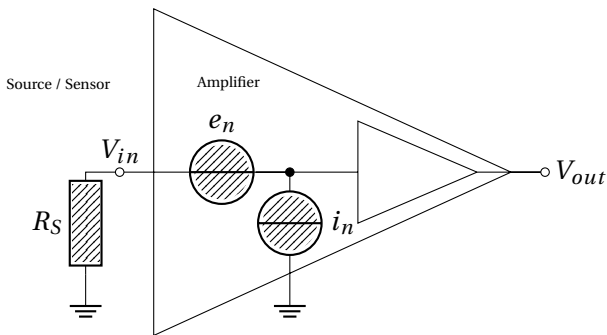
Noise synthesis

Nom	Forme	DSA S_i	Source
Johnson	white	$4k_B T/R$	Real resistance
shot	white	$2qI$	Junction
flicker	$1/f^\gamma$	$\frac{K}{A} \times \frac{I^\alpha}{f^\gamma}$	Semiconductor

Possible mitigations

- ▶ **Johnson** : Resistance, Température
- ▶ **shot** : Current
- ▶ **1/f** : Current density - size, technology/cleanliness

Noise Factor and Noise refer to the input (RTI)



Assuming a source resistance R_S and a voltage amplifier, the noise factor NF :

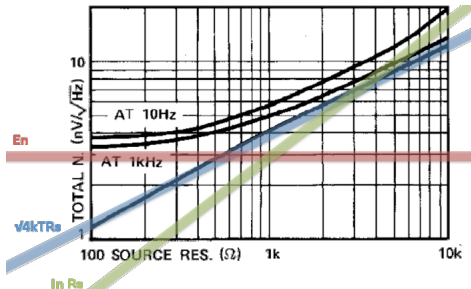
$$NF = 10 \log \frac{\frac{V_{in}^2}{4k_B T R_S}}{\frac{(G V_{in})^2}{G^2 (4k_B T R_S + e_n^2 + R_S^2 i_n^2)}} = 10 \log \frac{4k_B T R_S + e_n^2 + R_S^2 i_n^2}{4k_B T R_S}$$

≙ e_n^2 and i_n^2 here the spectral density and $G = \frac{V_{out}}{V_{in}}$ the voltage noise

Input noise vs source resistance

$$NF = 10 \log \frac{4k_B T R_S + e_n^2 + R_S^2 i_n^2}{4k_B T R_S}$$

Example: input noise *vs* optimal noise resistance of an OP27

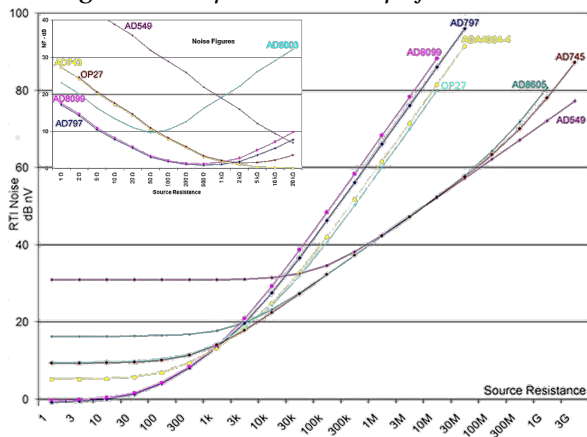


OP27 datasheet

When total noise is close the Johnson noise -> optimal source resistance (minimum NF)

Noise index *vs* source resistance

Analog Devices *operational amplifier noise*



- For a **low impedance** source -> AD797;

- For a **high impedance** source -> AD745.

- NOISE INDEX approaches 1 (0dB) for **Optimal impedance**

Optimal impedance $R_{S_{opt}}$

$R_{S_{opt}}$: source impedance R_S : NOISE INDEX

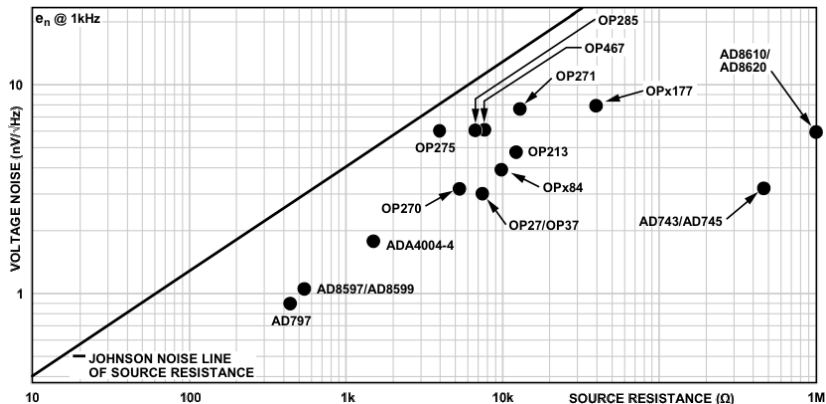
$$F_{min} \rightarrow \frac{\partial F}{\partial R_S} = 0 \Big|_{R_S=R_{S_{opt}}}$$

$$\frac{\partial \left(1 + \frac{R_{S_{opt}}^2 i_n^2 + e_n^2}{4k_B T R_{S_{opt}}} \right)}{\partial R_{S_{opt}}} = 0$$

$$\frac{i_n^2}{4k_B T} - \frac{e_n^2}{4k_B T R_{S_{opt}}^2} = 0 \rightarrow \boxed{R_{S_{opt}} = \frac{e_n}{i_n}}$$

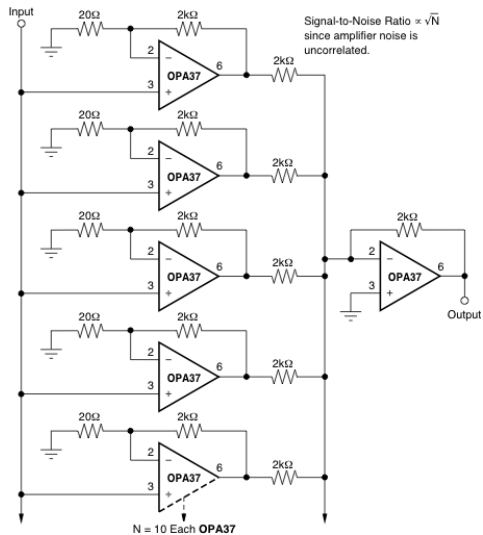
Aop Analog Devices en fonction de $R_{S_{opt}}$

Low Noise Amp. Selection Guide for Optimal Noise Perf.



P. Lee - A.D. Application Note

Decreasing noise by putting Aop in //



OPA27 datasheet

Quadratic sum of independent noise (multiplied by \sqrt{N}); **Signal** (same for all amplifier) **is multiply by N.**

The first non inverter stages provide N gains = 101 ($1 + 2k\Omega/20\Omega$); Last stage sum (sommer-inverter) :

Voltage gain = -1010

Cryogenic electronic devices

1. **Field-effect** Transistors - FET
 - ▶ standard MOS & JFET
 - ▶ Hetero-junction FET *ie* HEMT
2. **Bipolar** transistors
 - ▶ Bipolar Junction Transistor - BJT
 - ▶ Hetero-junction Bipolar Transistor - HBT
3. **Superconductor** devices
 - ▶ Superconducting QUantum Interference Devices - SQUIDs

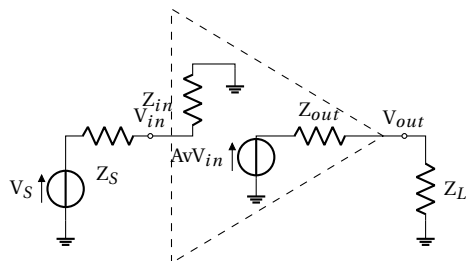
Amplifications and figures of merit

signal amplification

Input signal \Rightarrow **Gain** \Rightarrow **Output signal**

AMPLIFICATION	UNIT	EXEMPLES
voltage	[V/V]	transformer; op. amplifier
current	[A/A]	transfo.; bipolar trans. (β)
transimpedance	[V/A]; [Ω]	resistor, SQUID + input coil
transconductance	[A/V]; [S]	transistor (g_m)

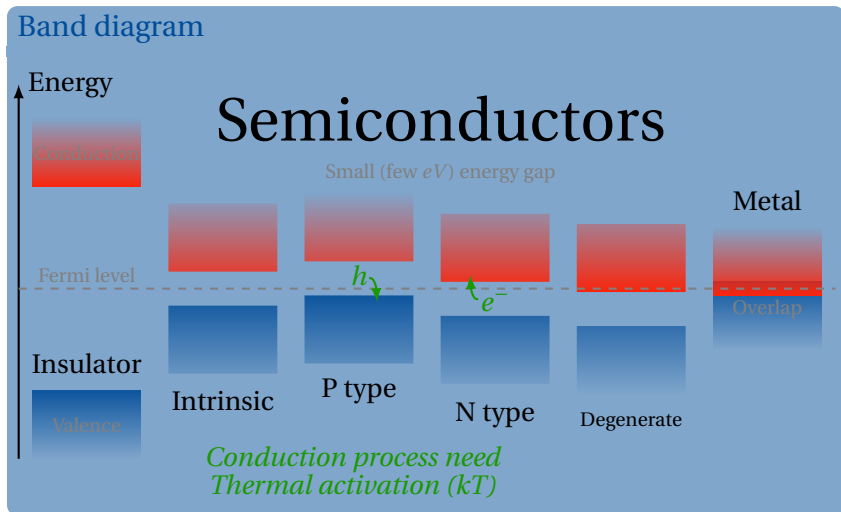
Voltage/Current sources and "matching" impedance



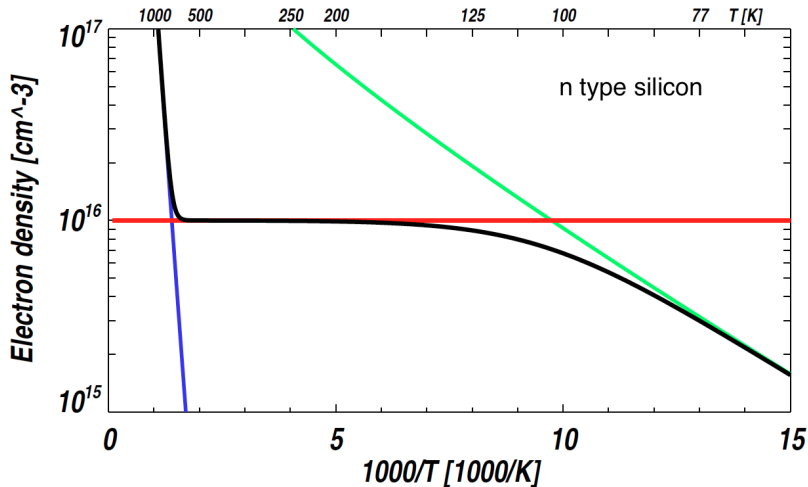
voltage amplifier example

AMPLIFICATION	INPUT	OUTPUT
voltage gain	$Z_{in} > Z_S$	$Z_L > Z_{out}$
current gain	$Z_{in} < Z_S$	$Z_L < Z_{out}$
transimpedance	$Z_{in} < Z_S$	$Z_L > Z_{out}$
transconductance	$Z_{in} > Z_S$	$Z_L < Z_{out}$

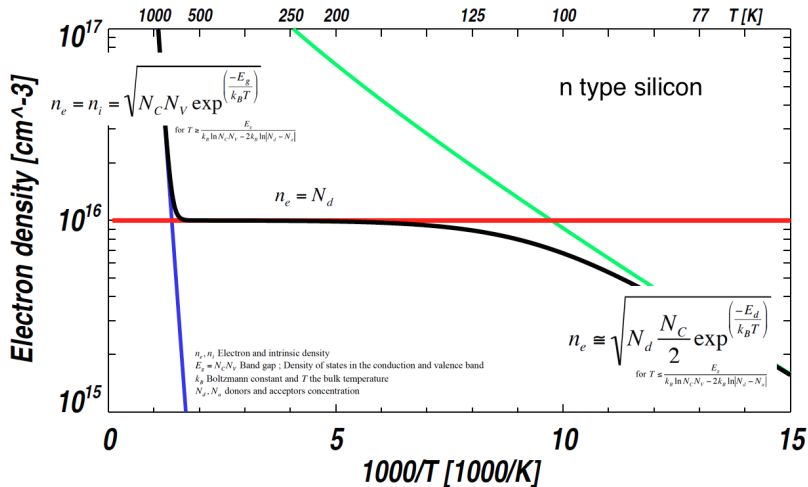
Solid-state physics and semiconductors



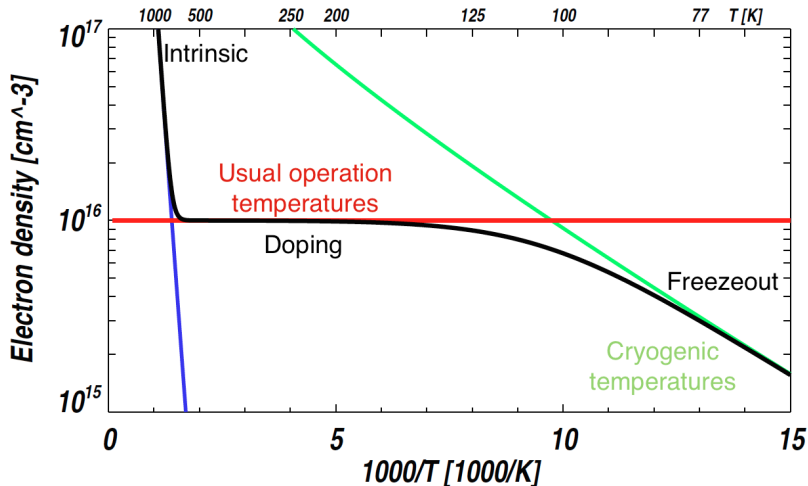
Solid-state physics and semiconductors (carriers density as function of T)



Solid-state physics and semiconductors (carriers density as function of T)



Solid-state physics and semiconductors (carriers density as function of T)



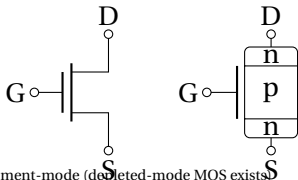
Field Effect Transistor - FET

Field effect transistor uses **ELECTRIC FIELD** to **control** the output current

Different ways to **isolate** the grid

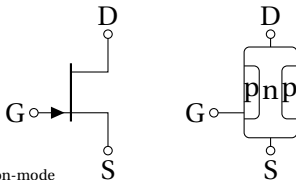
1. **INSULATOR** (as SiO₂)
→ MOSFET (Metal Oxide Semiconductor FET)
2. **Depleted region** of a reverse biased **pn JUNCTION**
→ JFET (Junction FET)
3. **Depleted wide band-gap** of an **HETEROSTRUCTURE** (as GaAs/AlGaAs)
→ HEMT (High Electron Mobility Transistor)

nMOS nodes & topology



enhancement-mode (depleted-mode MOS exists)

nJFET nodes & topology



depletion-mode

Parameters :▶ **transconductance**

$$g_m = \frac{\partial I_D}{\partial V_{GS}}$$

- ▶ capacitive input impedance \rightarrow close to ∞ at low freq.
- ▶ current gain not defined $\rightarrow Z_{IN}$ too large
- ▶ output impedance depends on the circuit (what the output is)

MOS and JFET transconductance

2 different operation modes for amplification

1. weak-inversion for low consumption;

$$I_D = I_{D0} \exp \frac{V_{GS} - V_{th}}{\eta V_T} \Rightarrow g_m = \frac{I_D}{\eta V_T}$$

$$I_{D0} = I_D \text{ and } V_{GS} = V_{th}, \eta = 1 + \frac{C_D}{C_{ox}} \text{ at}$$

$$V_T = \frac{k_B T}{q}$$

2. the **active mode** for low-noise analog amplifier

Linear low noise amplification \rightarrow *pinch-off* and **active mode** (saturation)

$$\blacktriangleright I_D(V_{DS}) \approx \kappa (V_{GS} - V_{th})^2 \text{ with } \kappa = \begin{cases} \frac{\mu C_{ox}}{2} \frac{W}{L} & \text{for MOS} \\ \frac{I_{DSS}}{V_{th}} & \text{for JFET} \end{cases}$$

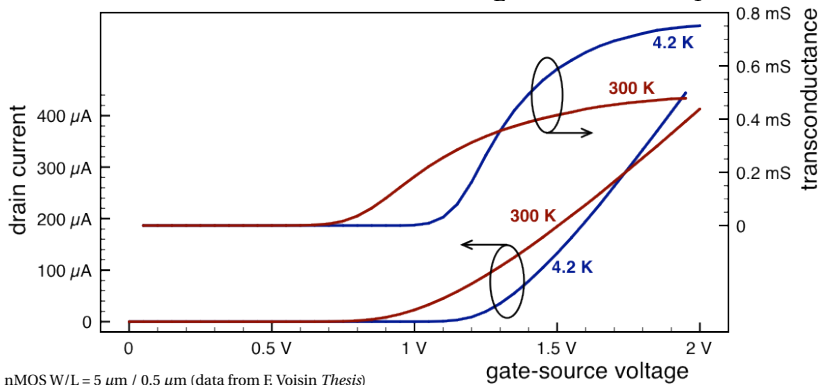
$$\blacktriangleright |g_m| = \left| \frac{\partial I_D}{\partial V_{GS}} \right| \approx \boxed{2\kappa (V_{GS} - V_{th})} \propto \sqrt{I_D}$$

$$\blacktriangleright \mu(T) \propto T^{-\alpha} \rightarrow \mu \nearrow \text{ at low temperature} \Rightarrow \boxed{g_m \propto \frac{\sqrt{I_D}}{T^\alpha}}$$

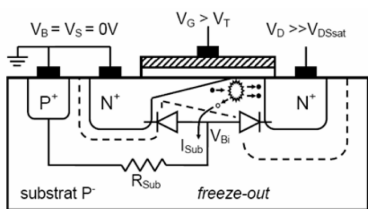
Cryogenic measurement of MOS transconductance

$$I_D(V_{DS}) \approx \frac{\mu C_{ox}}{2} \frac{W}{L} (V_{GS} - V_{th})^2$$

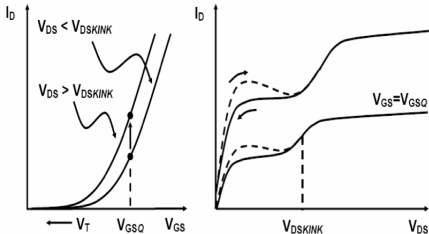
$$\Rightarrow |g_m| \approx \mu C_{ox} \frac{W}{L} (V_{GS} - V_{th}) \propto \frac{\sqrt{I_D}}{T^\alpha}$$



MOS output characteristic and *kink effect*



● electron ○ hole ⊙ electron collision with the ionic lattice



F. Voisin - "uElec. Cryo. pour instru. bas bruit", Porquerolles 2007

At high V_D , e^- -hole pairs created by impact ionization mechanism.

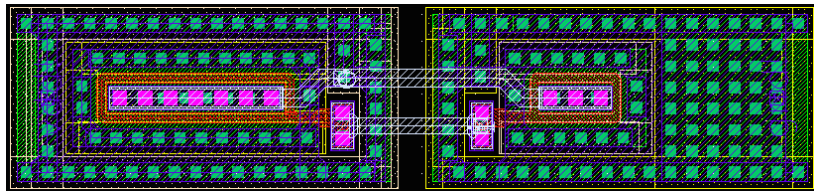
- ▶ $e^- \rightarrow$ drain
- ▶ holes stay in the frozen-out bulk (increasing the bulk potential)
 - \Rightarrow add a "potential control" in addition to V_{GS}

Kink effect is stronger in nMOS as compared to pMOS

Solution : adding many bulk contact around the MOS

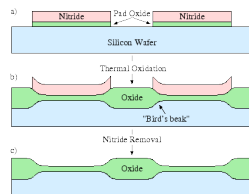
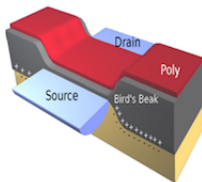
MOS transistor design for cryo. and space applications

To mitigate the kink effect, all MOS transistors are fully surrounded by substrat contacts (to really fix the potential) :



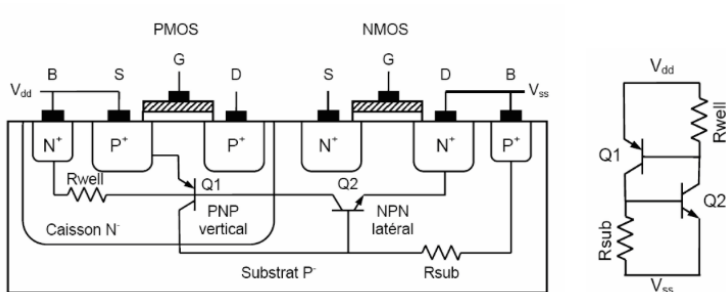
Example of inverter in AMS 0.35 Technology

Moreover, **ELT** (Edge-Less Transistors) suppress the effect of the charges trapped in "bird's beak" of standard MOS design (LOCAL Oxidation of Silicon)



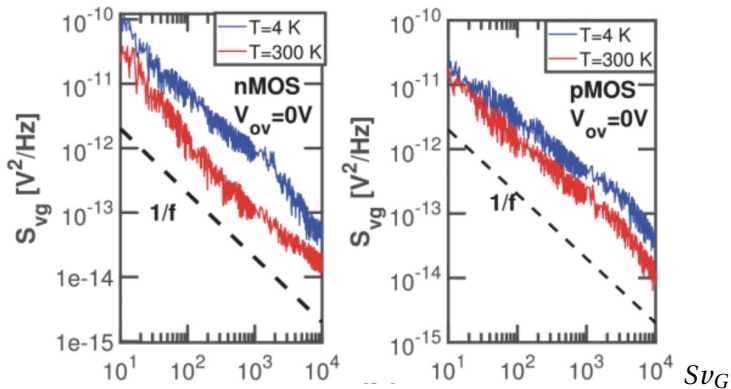
Latch-up mitigation at cryogenic temperatures

- ▶ Gard ring used to reduce kink effect allows to reduce too the Latch-up occurrence
- ▶ At low temperatures, freeze-out dramatically reduce BJT (Bipolar Junction Transistor) current gain



F. Voisin - "uElec. Cryo. pour instru. bas bruit", Porquerolles 2007

MOS transistor Flicker evolution with T



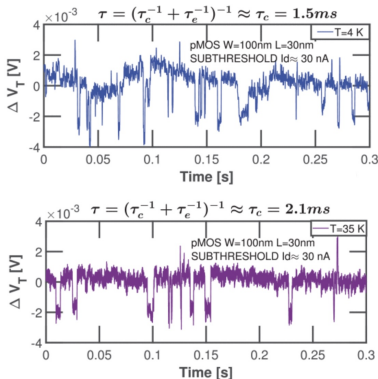
measurements 28nm technology (a) nMOS and (b) pMOS at 300 and 4 K for $V_{ov} = 0\text{ V}$ and $V_{ds} = 20\text{ mV}$. Notice that the noise amplitude at 4 K is higher than the one at 300 K

Ruben Asanovski et al. Understanding the

Excess 1/f Noise in MOSFETs at Cryogenic Temperatures - 2023

1/f noise excess at cryogenic temperature

- band tail states start to behave as traps at cryogenic temperatures
- related to the temperature dependence of the hopping mechanism in band tail states
- plus dielectric traps

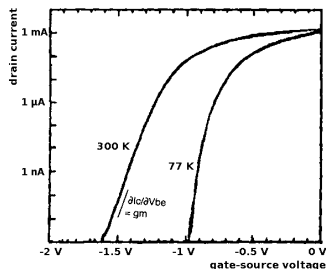


The trapping dynamics :

- > decrease in temperature reduce the number of traps thermally accessible, resulting in a noise spectrum originating from a few τ only

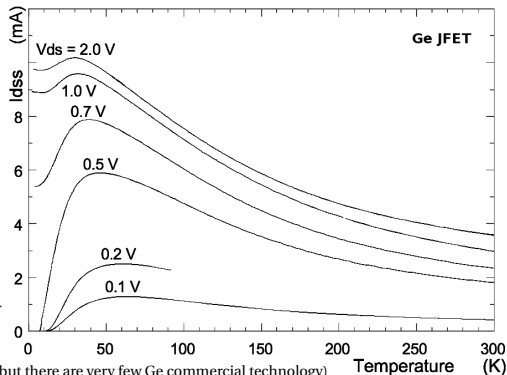
Cryogenic measurement of JFET transconductance

$$I_D(V_{DS}) \approx I_{DSS} \left(1 - \frac{V_{GS}}{V_{th}}\right)^2 \Rightarrow |g_m| \approx 2I_{DSS} \left(1 - \frac{V_{GS}}{V_{th}}\right) \propto \sqrt{I_D} I_{DSS}$$



Goldberg et al - Characterization of cryo Si JFET

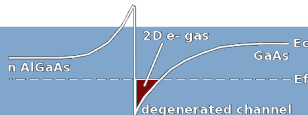
Ward et al - Dev. of Cryo Ge JFET ->



Si JFET for 77 K applications and Ge JFET for 4 K (but there are very few Ge commercial technology)

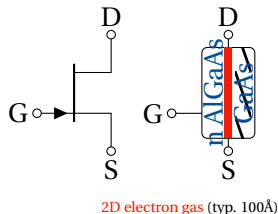
High Electron Mobility Transistor - HEMT

Charge carriers in 2D layer rather than created by dopants



AsGa HEMT nodes & topology

HEMT technologies (JFET with heterojunction)

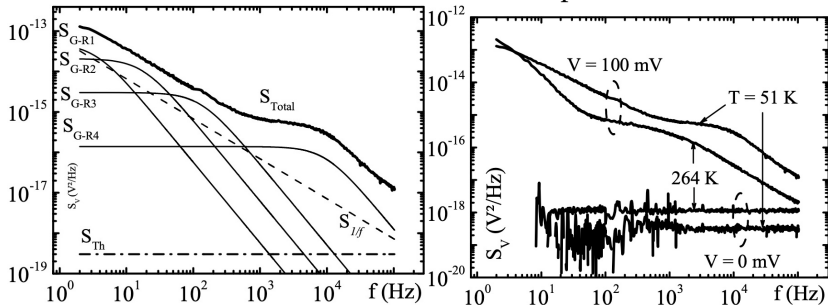


- ▶ **Very high e^- mobility** → high g_m
- ▶ High operation frequency up to mm wavelengths
- ▶ e^- conduction spatially separated from donor impurities → **no ionized scattering** (collisions with impurities)

- ▶ Allows operation down to **sub-Kelvin temperatures** (degenerated)

1/f Noise in a HEMT @ cryo T

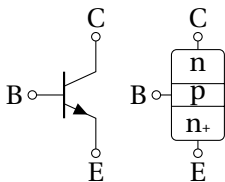
Typical decomposition of PSD at $T = 51$ K : Thermal noise (S_{Th}), 1/f noise ($S_{1/f}$) and one or several G-R noise components (S_{G-R}) :



S. Mouetsi et al, The 1/f Noise in a Two-Dimensional Electron Gas: Temperature and Electric Field Considerations

Noise in semiconductor is affected by various parameters such as conductivity, defect density, temperature, doping concentration, and bias voltage. However, when bias or temperature are varied, the semiconductor properties are no longer constant ... when the temperature is lowered, a shift of the cutoff frequencies towards lower values occurs, new levels appear

Nodes & topology



Bipolar transistor technologies

Thin semiconductor material common to 2 junctions :

- ▶ **Homojunctions** Si/Si
→ Bipolar Junction Transistor - **BJT**
- ▶ **Heterostructure** III/V as InP/InGaAs or IV/IV as Si/SiGe
→ Heterojunction Bipolar Trans. - **HBT**

Parameters :

- ▶ **transconductance**
- ▶ **current gain**
- ▶ **input impedance**

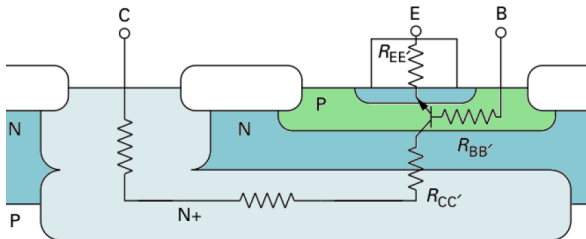
$$g_m = \frac{\partial I_C}{\partial V_{BE}}$$

$$\beta = \frac{\partial I_C}{\partial I_B}$$

$$h_{11} = \frac{\partial V_{BE}}{\partial I_B} = \frac{\beta}{g_m}$$

Bipolar access resistances R'

At cryogenic temperatures, weakly doped semiconductor suffer from freeze-out \Rightarrow **increasing of the access resistances**

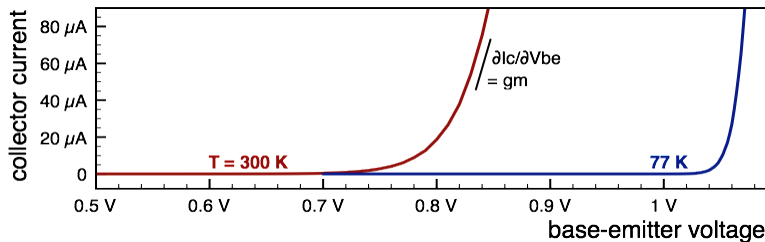


$R_{BB'}$ and $R_{EE'}$ access resistances are **combine in a unique R'**

$$R' = \frac{R_{BB'}}{\beta} + \frac{(\beta + 1)R_{EE'}}{\beta}$$

Transconductance - g_m

Drift diffusion theory $I_C = I_{C0} \exp \frac{V_{BE}}{V_T}$ with $V_T = \frac{k_B T}{q}$



recombinations, carrier mean free path, thermal decoupling and R'

$$g_m = \frac{\partial I_C}{\partial V_{BE}} = \frac{I_C}{V_T} = \frac{q I_C}{k_B T} \quad \Rightarrow \quad g_m \Big|_{T_{cryo}} = \frac{\frac{q I_C}{\eta k_B T_e}}{1 + R' \frac{q I_C}{\eta k_B T_e}}$$

Current gain β and input impedance

Degraded BJT current gain at low temperatures

$$\beta \propto \exp \frac{\Delta E_g}{k_B T} \quad \text{with} \quad \Delta E_g = E_{gE} - E_{gB} < 0$$

ΔE_g : difference in band gap between the emitter and the base regions and induced by **doping** - **band gap narrowing**

Example of common commercial transistor : 2N2222 BJT

measured β go from **225** to **35** from room temperature to 77 K

$$\underline{h_{11} = \frac{\beta}{g_m} :}$$

$$\text{Considering } I_C = 1 \text{ mA} \rightarrow h_{11(T=300\text{K})} = \frac{225}{39 \text{ mS}} \approx 6 \text{ k}\Omega$$

$$h_{11(T=77\text{K})} = \frac{35}{150 \text{ mS}} < 250 \Omega \quad \Rightarrow \quad \text{fails} \quad Z_{in} > Z_S \text{ at lower temperatures}$$

Heterojunction Bipolar Transistor - HBT

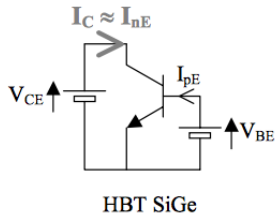
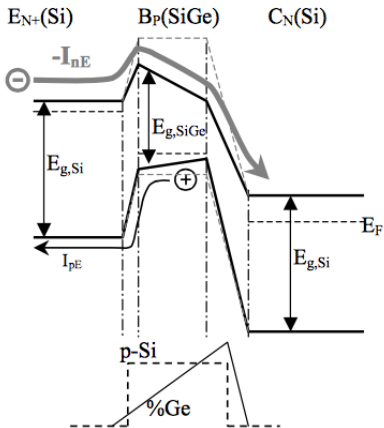
Differing semiconductor materials \implies Heterojunction

of one, at least, of the junctions of a bipolar transistor

\rightarrow **high frequency performances**

- ▶ **III-V or IV-IV hetero-junctions** are used by using InP/InGaAs or **Si/SiGe** for instance.
- ▶ Si/SiGe is one of the few hetero-junction **compatible with standard Si based technology**
SiGe HBT becomes the most popular bipolar technology with competitive speed, and even better, than III-V expensive technologies

HBT planar technology



Instru. Cryo. SiGe - PhD D. Prêle

SiGe and Cryogeny

- ▶ HBT is usually developed to achieve **high frequencies** perf.
- ▶ For **Cryogenic** applications, alloy of silicon and germanium (SiGe)

⇒ Change the $\beta(T)$

⇒ Pushes the **freeze-out** at lower temperatures

Si/SiGe heterojunction improve the **emitter injection efficiency**, as compare to BJT, so that it is possible to **increase the base doping**
 ⇒ **SiGe HBT still work at 4.2 K**, far away temperatures where Si BJT is freezed out

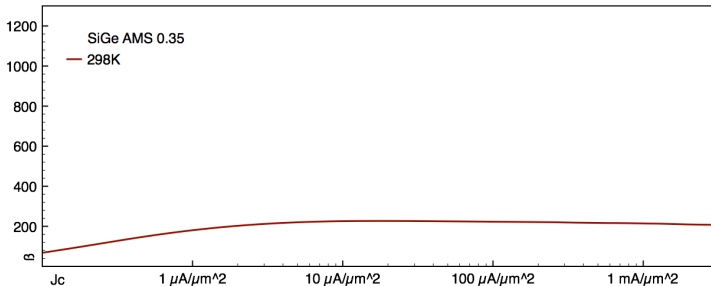
$$\beta_{HBT, SiGe} = \frac{\mu_n L_p N_{dE}}{\mu_p W_B N_{aB}} \exp \frac{\Delta E_{gSi/SiGe} - \Delta E_{gEapp}}{k_B T}$$

$$\beta_{BJT, Si} \approx \frac{\mu_n L_p N_{dE}}{\mu_p W_B N_{aB}} \exp \frac{-\Delta E_{gEapp}}{k_B T}$$

HBT current gain could increase exponentially with decreasing temperature

$$\beta_{SiGe} \propto \exp \frac{\Delta E_g}{k_B T} \quad \text{with} \quad \Delta E_g = \underbrace{E_{gE} - E_{gB}}_{<0 \text{ for BJT due to doping}} \approx \underbrace{E_{gESi} - E_{gBSiGe}}_{\text{could be } >0 \text{ due to Ge}}$$

$\beta(T)$ and "band gap *vs* doping"



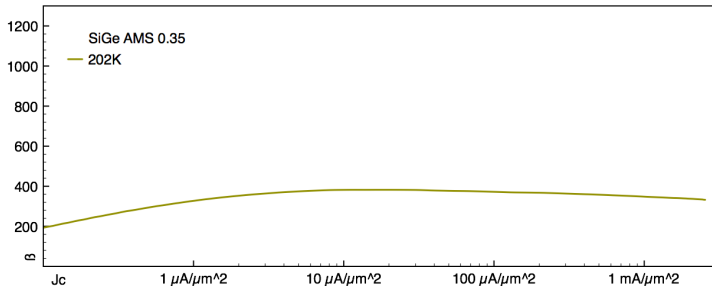
- ▶ at small J_C : recombinations in the base
- ▶ at large J_C : high injection

$$\beta(J_C) \xrightarrow{T \searrow} \text{"bell curve"}$$

HBT current gain could increase exponentially with decreasing temperature

$$\beta_{SiGe} \propto \exp \frac{\Delta E_g}{k_B T} \quad \text{with} \quad \Delta E_g = \underbrace{E_{gE} - E_{gB}}_{<0 \text{ for BJT due to doping}} \approx \underbrace{E_{gESi} - E_{gBSiGe}}_{\text{could be } >0 \text{ due to Ge}}$$

$\beta(T)$ and "band gap *vs* doping"



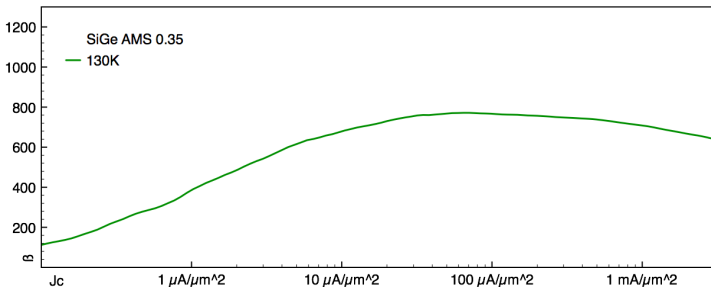
- ▶ at small J_C : recombinations in the base
- ▶ at large J_C : high injection

$$\beta(J_C) \xrightarrow{T \searrow} \text{"bell curve"}$$

HBT current gain could increase exponentially with decreasing temperature

$$\beta_{SiGe} \propto \exp \frac{\Delta E_g}{k_B T} \quad \text{with} \quad \Delta E_g = \underbrace{E_{gE} - E_{gB}}_{<0 \text{ for BJT due to doping}} \approx \underbrace{E_{gE_{Si}} - E_{gB_{SiGe}}}_{\text{could be } >0 \text{ due to Ge}}$$

$\beta(T)$ and "band gap *vs* doping"



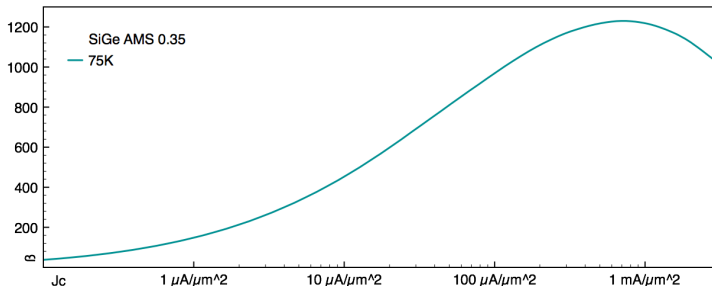
- ▶ at small J_C : recombinations in the base
- ▶ at large J_C : high injection

$$\beta(J_C) \xrightarrow{T \searrow} \text{"bell curve"}$$

HBT current gain could increase exponentially with decreasing temperature

$$\beta_{SiGe} \propto \exp \frac{\Delta E_g}{k_B T} \quad \text{with} \quad \Delta E_g = \underbrace{E_{gE} - E_{gB}}_{<0 \text{ for BJT due to doping}} \approx \underbrace{E_{gESi} - E_{gBSiGe}}_{\text{could be } >0 \text{ due to Ge}}$$

$\beta(T)$ and "band gap *vs* doping"



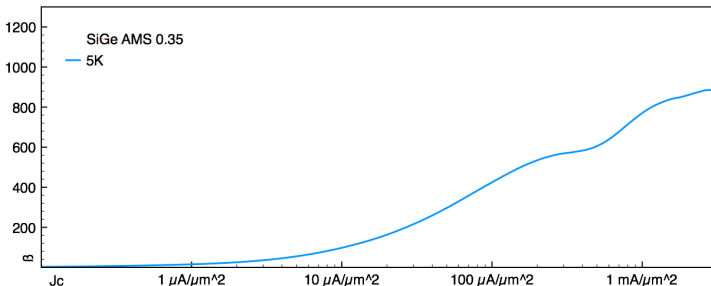
- ▶ at small J_C : recombinations in the base
- ▶ at large J_C : high injection

$$\beta(J_C) \xrightarrow{T \searrow} \text{"bell curve"}$$

HBT current gain could increase exponentially with decreasing temperature

$$\beta_{SiGe} \propto \exp \frac{\Delta E_g}{k_B T} \quad \text{with} \quad \Delta E_g = \underbrace{E_{gE} - E_{gB}}_{<0 \text{ for BJT due to doping}} \approx \underbrace{E_{gE_{Si}} - E_{gB_{SiGe}}}_{\text{could be } >0 \text{ due to Ge}}$$

$\beta(T)$ and "band gap *vs* doping"



- ▶ at small J_C : recombinations in the base
- ▶ at large J_C : high injection

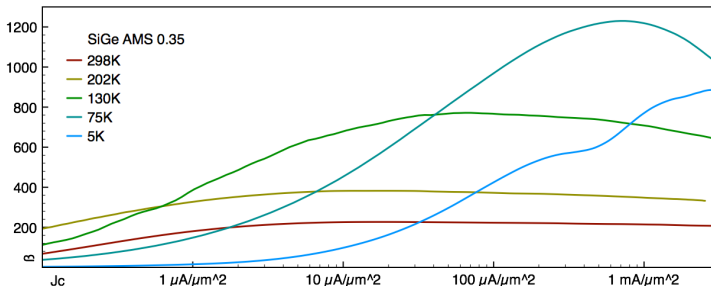
$\beta(J_C) \xrightarrow{T \searrow}$ "bell curve"

HBT current gain

could increase exponentially with decreasing temperature

$$\beta_{SiGe} \propto \exp \frac{\Delta E_g}{k_B T} \quad \text{with} \quad \Delta E_g = \underbrace{E_{gE} - E_{gB}}_{<0 \text{ for BJT due to doping}} \approx \underbrace{E_{gESi} - E_{gBSiGe}}_{\text{could be } >0 \text{ due to Ge}}$$

$\beta(T)$ and "band gap *vs* doping"



- ▶ at small J_C : recombinations in the base
- ▶ at large J_C : high injection

$$\beta(J_C) \xrightarrow{T \searrow} \text{"bell curve"}$$

HBT transconductance

As for, BJT, the SiGe HBT transconductance follows

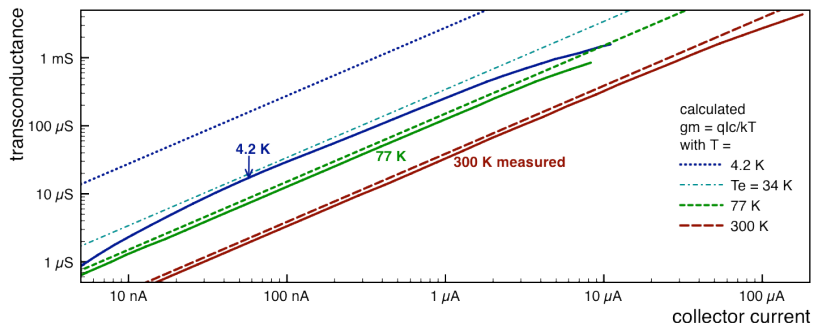
$$g_m = \frac{\frac{qI_C}{\eta k_B T_e}}{1 + R' \frac{qI_C}{\eta k_B T_e}} \quad \text{with} \quad R' = \frac{R_{BB'}}{\beta} + \frac{(\beta+1)R_{EE'}}{\beta}$$



Below 77 K, the HBT still operates ...

- ▶ Strong T_e decoupling
- ▶ "Start" of freeze-out $\Rightarrow R' \nearrow$
- ▶ R' effect if $R' \frac{qI_C}{\eta k_B T_e}$ is comparable or larger than 1
 - ▶ Large R'
 - ▶ Large I_C
 - ▶ Low T

measured SiGe transconductance

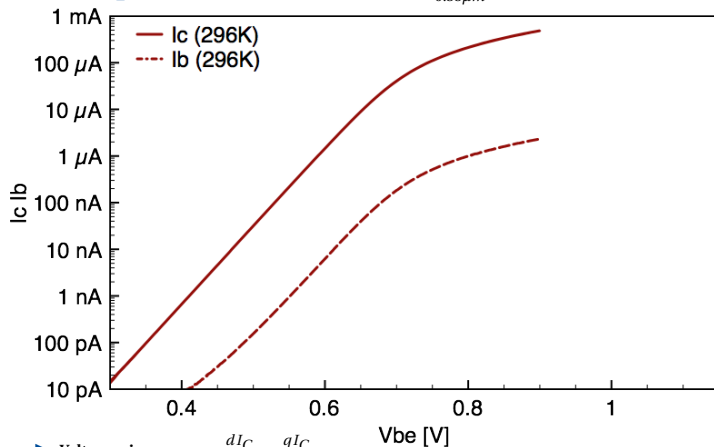


non-idealities

- ▶ $T_e \rightarrow$ the 4.2 K measurement fit with $qI_C/k_B 34$ K
- ▶ R' reduce the measured g_m (as compare to the ideal law)
- ▶ Recombination in the base-emitter depletion region at cryo. T

HBT parameters determined from pummel plots

Gummel plot of a NPN254 SiGe $AMS_{0.35\mu m}$ ($L_E = 50\mu m \rightarrow area = 20\mu m^2$)

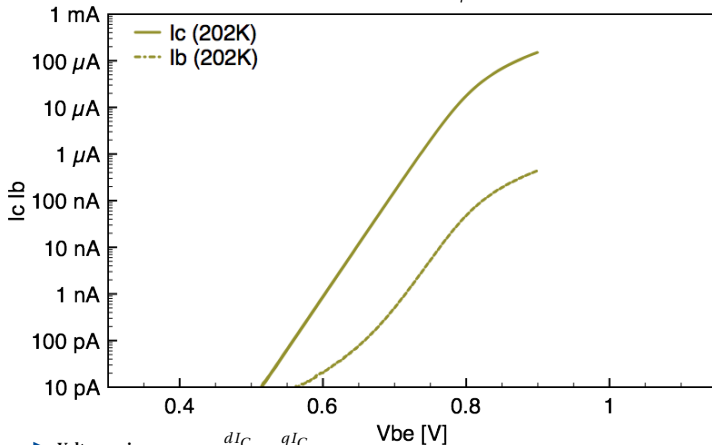


▶ Voltage gain $\Rightarrow g_m = \frac{dI_C}{dV_{be}} \approx \frac{qI_C}{k_B T}$

▶ Input impedance $\Rightarrow h_{11} = \frac{\beta}{g_m}$ and $\beta = \frac{I_C}{I_B}$; Buffer output impedance $\Rightarrow \frac{1}{g_m}$

HBT parameters determined from pummel plots

Gummel plot of a NPN254 SiGe AMS_{0.35}μm ($L_E = 50\mu\text{m} \rightarrow \text{area} = 20\mu\text{m}^2$)

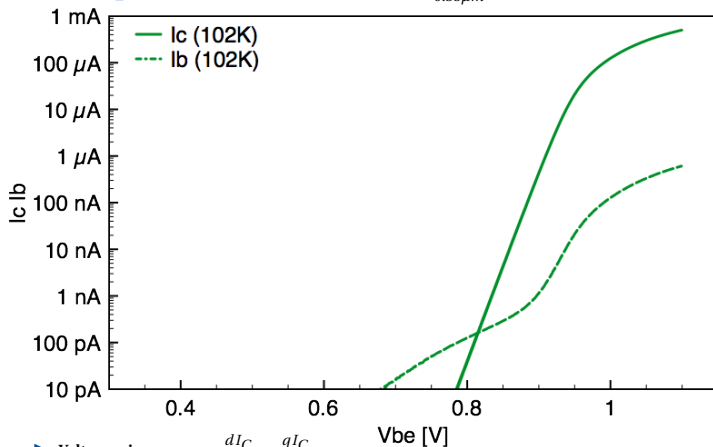


▶ Voltage gain $\Rightarrow g_m = \frac{dI_C}{dV_{be}} \approx \frac{qI_C}{k_B T}$

▶ Input impedance $\Rightarrow h_{11} = \frac{\beta}{g_m}$ and $\beta = \frac{I_C}{I_B}$; Buffer output impedance $\Rightarrow \frac{1}{g_m}$

HBT parameters determined from pummel plots

Gummel plot of a NPN254 SiGe_{AMS0.35 μ m} ($L_E = 50\mu\text{m} \rightarrow \text{area} = 20\mu\text{m}^2$)

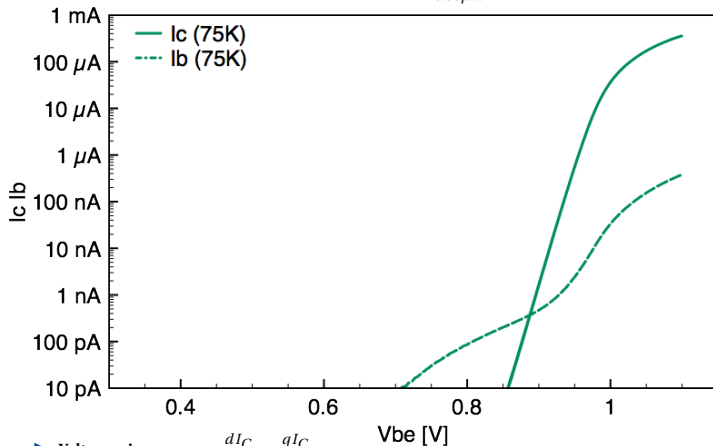


▶ Voltage gain $\Rightarrow g_m = \frac{dI_C}{dV_{be}} \approx \frac{qI_C}{k_B T}$

▶ Input impedance $\Rightarrow h_{11} = \frac{\beta}{g_m}$ and $\beta = \frac{I_C}{I_B}$; Buffer output impedance $\Rightarrow \frac{1}{g_m}$

HBT parameters determined from pummel plots

Gummel plot of a NPN254 SiGe_{AMS0.35 μ m} ($L_E = 50\mu\text{m} \rightarrow \text{area} = 20\mu\text{m}^2$)

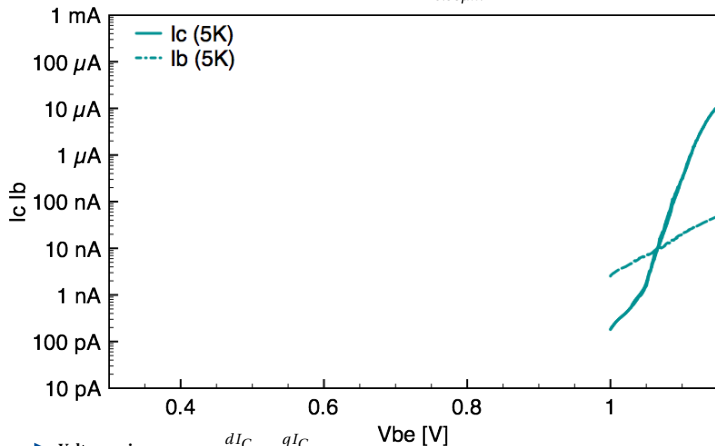


▶ **Voltage gain** $\Rightarrow g_m = \frac{dI_C}{dV_{be}} \approx \frac{qI_C}{k_B T}$

▶ **Input impedance** $\Rightarrow h_{11} = \frac{\beta}{g_m}$ and $\beta = \frac{I_C}{I_B}$; **Buffer output impedance** $\Rightarrow \frac{1}{g_m}$

HBT parameters determined from pummel plots

Gummel plot of a NPN254 SiGe_{AMS0.35 μ m} ($L_E = 50\mu\text{m} \rightarrow \text{area} = 20\mu\text{m}^2$)

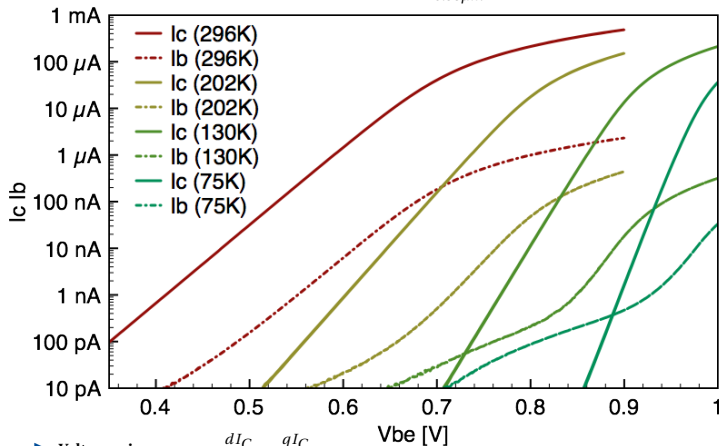


▶ **Voltage gain** $\Rightarrow g_m = \frac{dI_C}{dV_{be}} \approx \frac{qI_C}{k_B T}$

▶ **Input impedance** $\Rightarrow h_{11} = \frac{\beta}{g_m}$ and $\beta = \frac{I_C}{I_B}$; **Buffer output impedance** $\Rightarrow \frac{1}{g_m}$

HBT parameters determined from pummel plots

Gummel plot of a NPN254 SiGe_{AMS0.35μm} ($L_E = 50\mu\text{m} \rightarrow \text{area} = 20\mu\text{m}^2$)



▶ Voltage gain $\Rightarrow g_m = \frac{dI_C}{dV_{be}} \approx \frac{qI_C}{k_B T}$

▶ Input impedance $\Rightarrow h_{11} = \frac{\beta}{g_m}$ and $\beta = \frac{I_C}{I_B}$; Buffer output impedance $\Rightarrow \frac{1}{g_m}$

Calculated h_{11} from β and g_m measurements

input impedance h_{11}

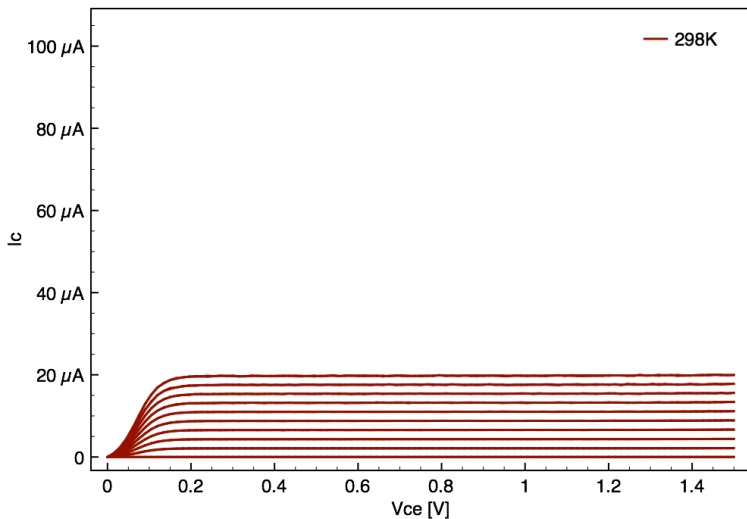
$$h_{11} = \frac{\beta}{g_m}$$

Considering a HBT SiGe with $100 \mu\text{m}^2$ area and $I_C = 1 \text{ mA}$

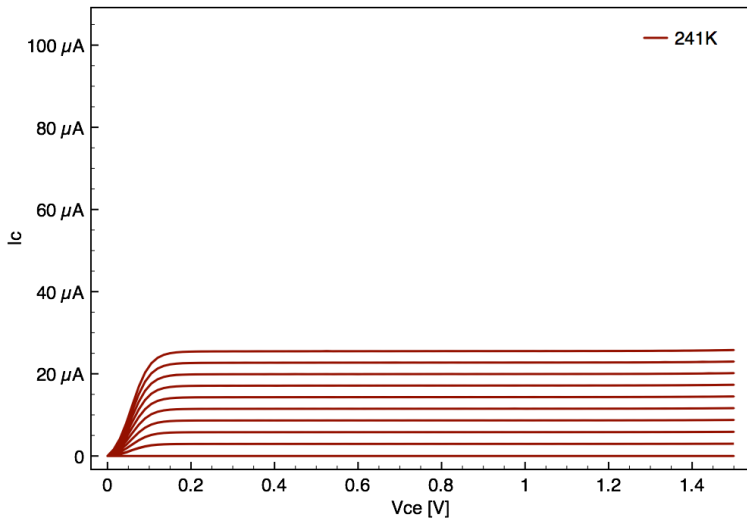
- ▶ J_C is thus equal to $10 \mu\text{A}/\mu\text{m}^2$ ($1 \text{ mA}/100 \mu\text{m}^2$)

Parameters	300 K	77 K	4.2 K
β	180	1400	900
g_m	30 mS	100 mS	150 mS
h_{11}	6 k Ω	14 k Ω	6 k Ω

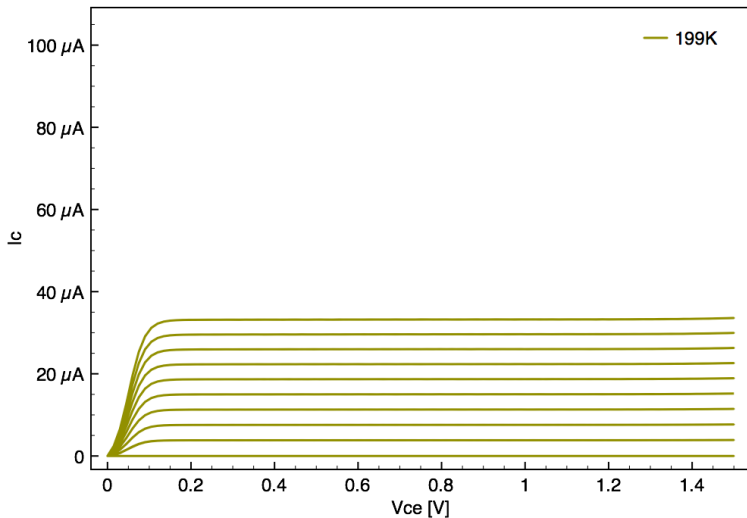
HBT $I_c(V_{ce})$ characteristic $\rightarrow V_{ce}$ offset



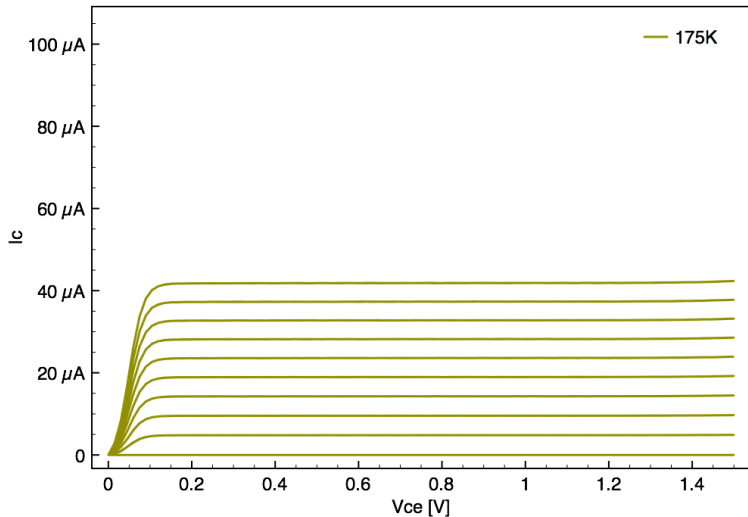
HBT $I_c(V_{ce})$ characteristic $\rightarrow V_{ce}$ offset



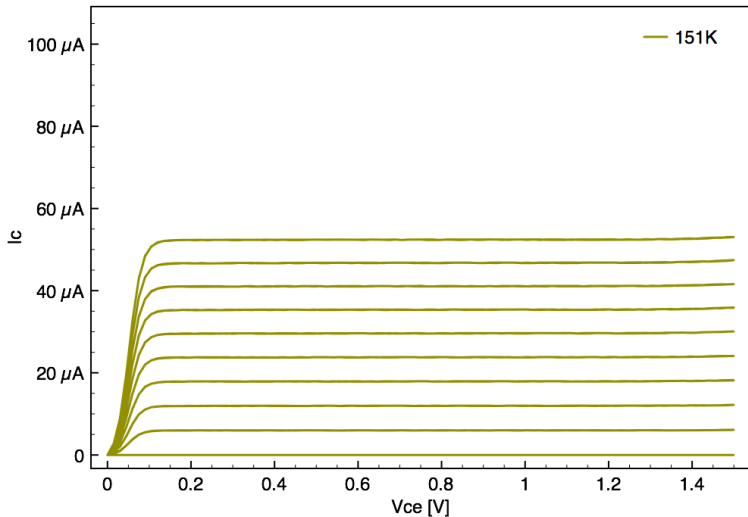
HBT $I_c(V_{ce})$ characteristic $\rightarrow V_{ce}$ offset



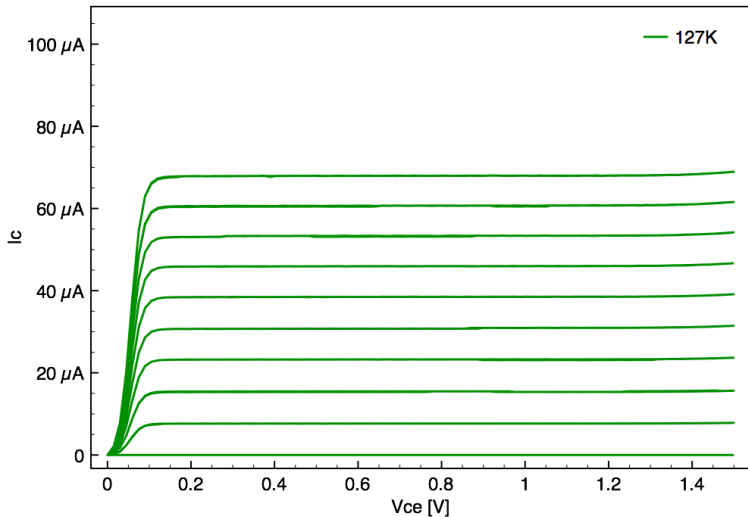
HBT $I_c(V_{ce})$ characteristic $\rightarrow V_{ce}$ offset



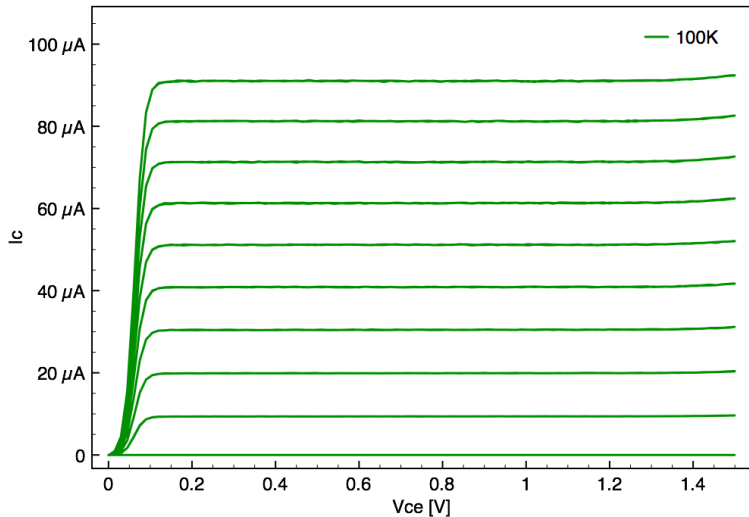
HBT $I_c(V_{ce})$ characteristic $\rightarrow V_{ce}$ offset



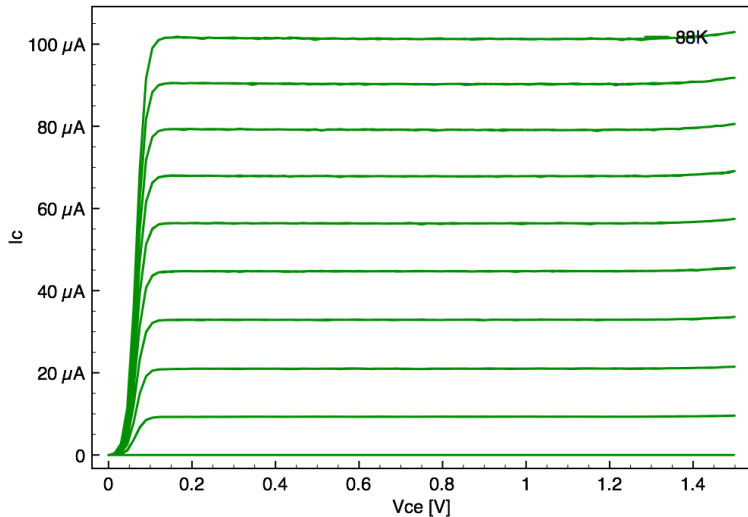
HBT $I_c(V_{ce})$ characteristic $\rightarrow V_{ce}$ offset



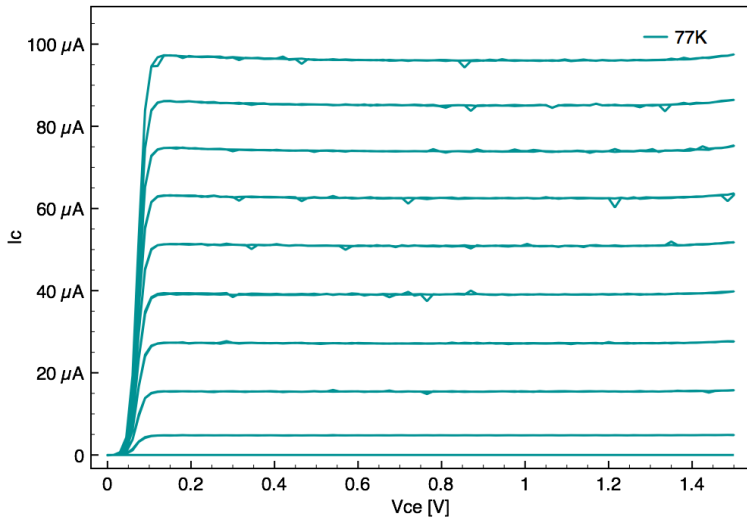
HBT $I_c(V_{ce})$ characteristic $\rightarrow V_{ce}$ offset



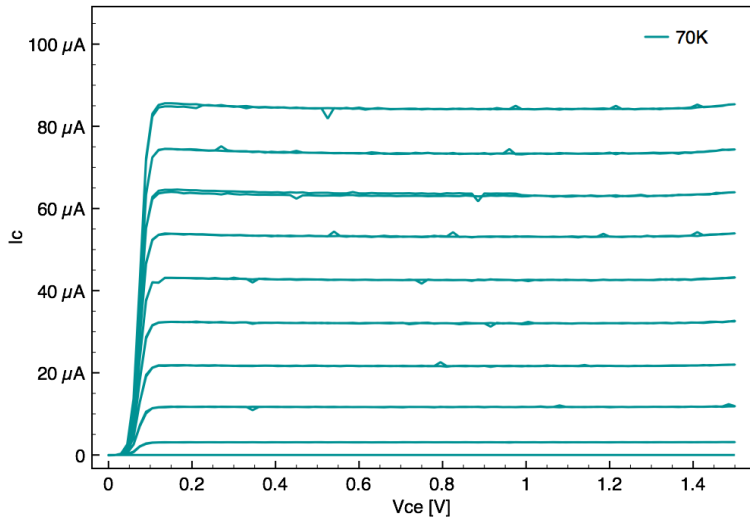
HBT $I_c(V_{ce})$ characteristic $\rightarrow V_{ce}$ offset



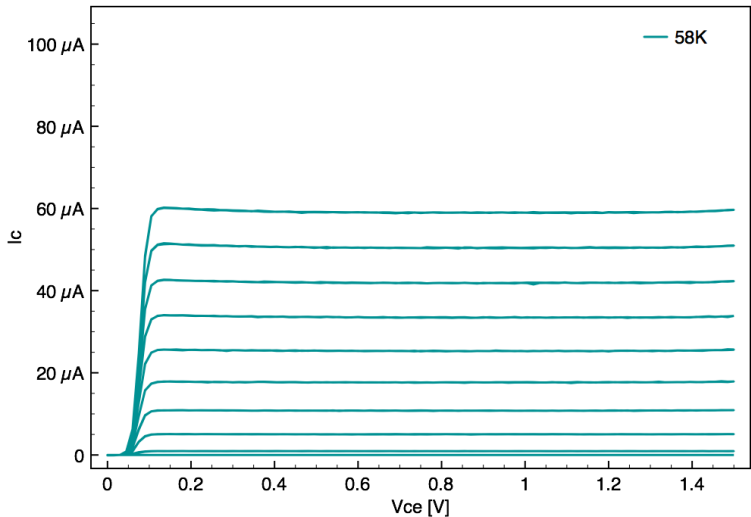
HBT $I_c(V_{ce})$ characteristic $\rightarrow V_{ce}$ offset



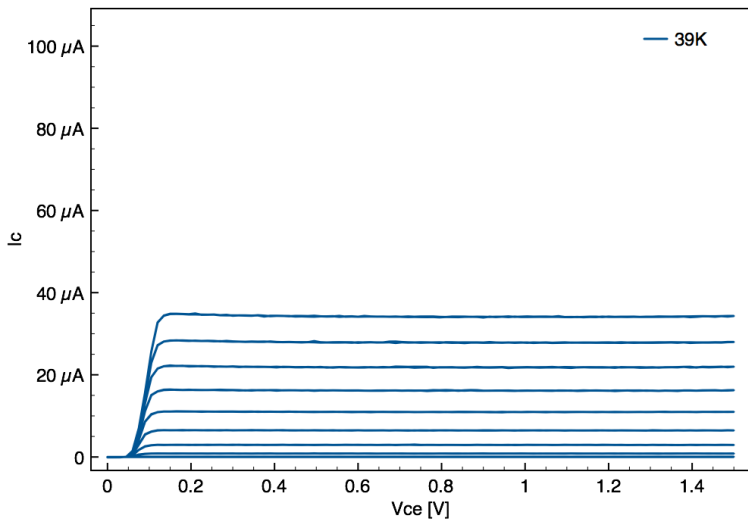
HBT $I_c(V_{ce})$ characteristic $\rightarrow V_{ce}$ offset



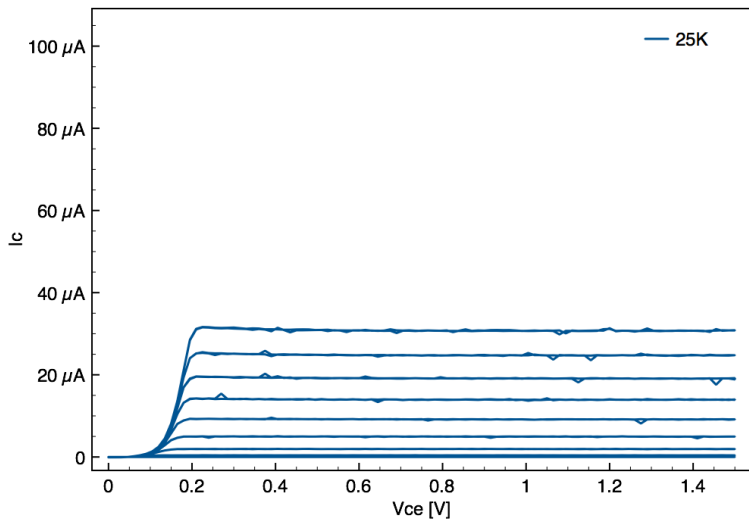
HBT $I_c(V_{ce})$ characteristic $\rightarrow V_{ce}$ offset



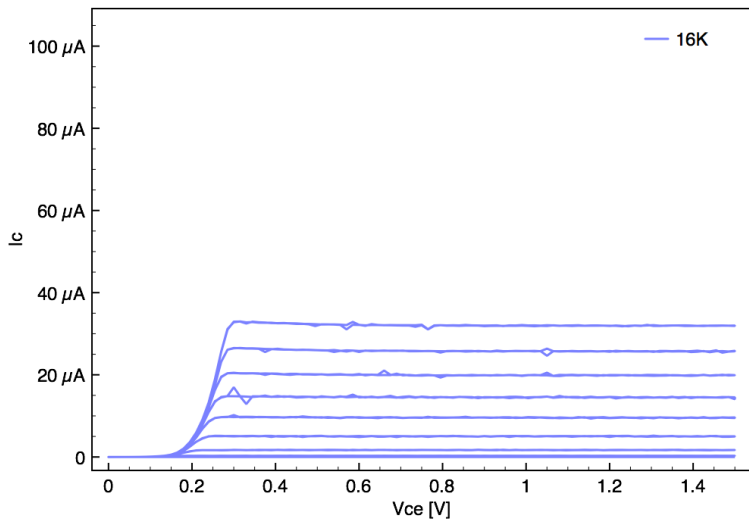
HBT $I_c(V_{ce})$ characteristic $\rightarrow V_{ce}$ offset



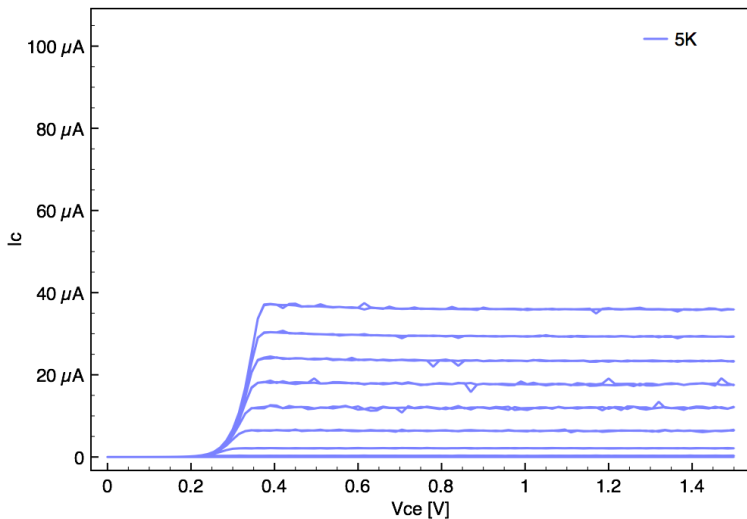
HBT $I_c(V_{ce})$ characteristic $\rightarrow V_{ce}$ offset



HBT $I_c(V_{ce})$ characteristic $\rightarrow V_{ce}$ offset



HBT $I_c(V_{ce})$ characteristic $\rightarrow V_{ce}$ offset



Noise discussion - on the benefit to have the larger g_m

FET noise = THERMAL noise of the channel resistance

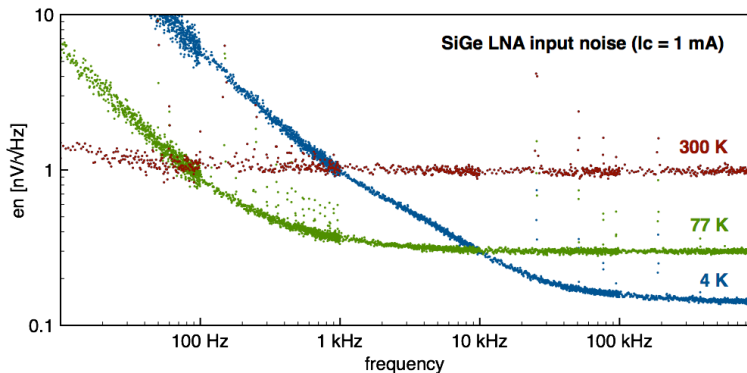
- ▶ Output current noise : $S_{i_D} = 4k_B T \frac{2g_m}{3} + K \frac{I_D^{\alpha \approx 2}}{f^{\gamma \approx 1}}$
- ▶ **Input voltage noise** : $S_{v_{GS}} = \frac{S_{i_D}}{g_m^2} = \frac{8k_B T}{3g_m} + \frac{K}{g_m^2} \frac{I_D^{\alpha \approx 2}}{f^{\gamma \approx 1}}$

Bipolar noise = SHOT noise of the junctions

- ▶ **Input voltage noise** $S_{v_{BE}} = 4k_B T R_{BB'} + \frac{2qI_C}{g_m^2} + K \frac{R_{BB'} I_B^{\alpha \approx 2}}{f^{\gamma \approx 1}}$
 $\approx \frac{4k_B T}{2g_m} + K \frac{R_{BB'} I_B^{\alpha \approx 2}}{f^{\gamma \approx 1}}$
- ▶ Input current noise $S_{i_B} = 2qI_B + K \frac{I_B^{\alpha \approx 2}}{f^{\gamma \approx 1}}$

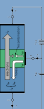
SiGe HBT Shot noise and 1/f (?) noise at cryo. T

1/f noise

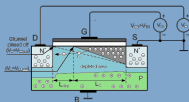


$$e_n \approx \frac{\sqrt{2qI_C}}{g_m} \quad \text{with} \quad g_m \approx \frac{qI_C}{k_B T} \Rightarrow I_C \text{ fixed by the required input noise}$$

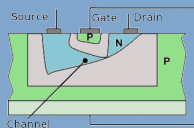
1/f noise and transistor topology



1/f noise is essentially due to the **non-ideal base current** in bipolar technologies



for MOS its cause come from the **trap on the oxide/channel interface** at the surface of the substrate



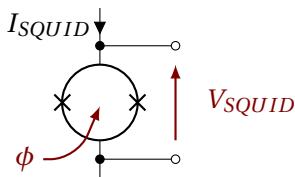
JFET channel is geometrically limited only by depleted regions → Less trap than near the surface → **Low 1/f noise**

+ effect of the size → $1/f \propto 1/Area$

Superconducting QUantum Interference Device

SQUID = Magnetic flux transducer \Rightarrow Voltage

The "DC SQUID" is composed of one superconducting ring (*Washer*) interrupted by two Josephson junctions (x).



Very sensitive magnetometer which combine two physical phenomena :

1. **Magnetic flux quantization** ($\phi_0 = \frac{h}{2e} \approx 2.10^{-15} \text{ Wb ou } [T.m^2] \text{ ou } [V.s]$) **in a superconducting loop**
2. **Josephson tunneling effect**

$h \approx 6,6.10^{-34} \text{ J.s or } [W.s^2]$ Planck constant; $e \approx 1,6.10^{-19} \text{ C or } [A.s]$

Magnetic flux quantization in a superconducting ring

Quantum properties of the superconductivity : $q = 2e$ (charge of the Cooper pair)

Superconductor is described by a **quantum wave function** ψ .

In superconducting ring, phase of ψ continuously change but **must comes to the same value around a turn** → magnetic flux screening can only compensates n magnetic flux quanta ϕ_0 :



$$\phi = n \frac{h}{2e} = n\phi_0$$

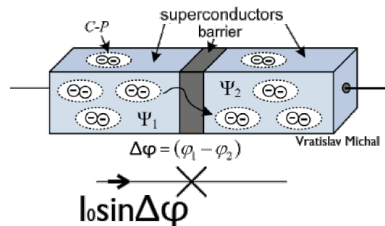
$\phi_0 = \frac{h}{2e} \approx 2.10^{-15} \text{ Wb}$ ou $[\text{T.m}^2]$ ou $[\text{V.s}]$ le quantum de flux magnétique

Josephson junction

2 superconductors separated by a thin ($\approx 10\text{nm}$) non-superconducting barrier.

Josephson tunneling effect :

Cooper pairs of electrons pass through the barrier by tunneling effect, maintaining phase coherence in the process.



Current biasing controls **phase difference $\Delta\phi$ between the two superconductor** according $I = I_0 \sin \Delta\phi$ leading to superconducting **phase modulation**.

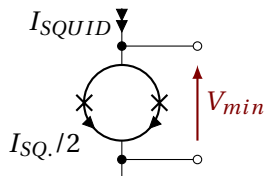
Interferences

For $I > I_0 \Rightarrow$ **voltage across the junction became >0**

Superconducting phase difference evolves with time at the
 \rightarrow **Josephson frequency :**

$$I \approx I_0 \sin\left(2\pi \frac{V}{\phi_0} t\right) \Rightarrow \frac{f}{V} = \frac{1}{\phi_0} \approx 500 \text{MHz}/\mu\text{V}$$

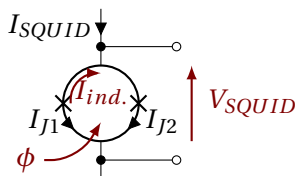
SQUID provides at low frequency, average value of interferences.



**With no magnetic flux, the 2 junctions oscillate in phase
 \Rightarrow destructive interference.**

Flux and superconducting phase shift

Magnetic flux leads to an additional phase shift $2\pi \frac{\phi}{\phi_0}$



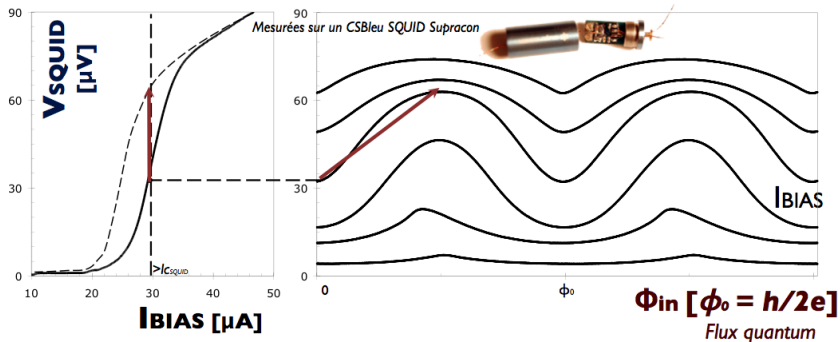
$$I_{J1} \approx I_0 \sin \left(2\pi \frac{V}{\phi_0} t - 2\pi \frac{\phi}{\phi_0} \right)$$

$$I_{J2} \approx I_0 \sin \left(2\pi \frac{V}{\phi_0} t + 2\pi \frac{\phi}{\phi_0} \right)$$

The two junctions are not in phase for $\phi \neq n\phi_0$ (periodicity)

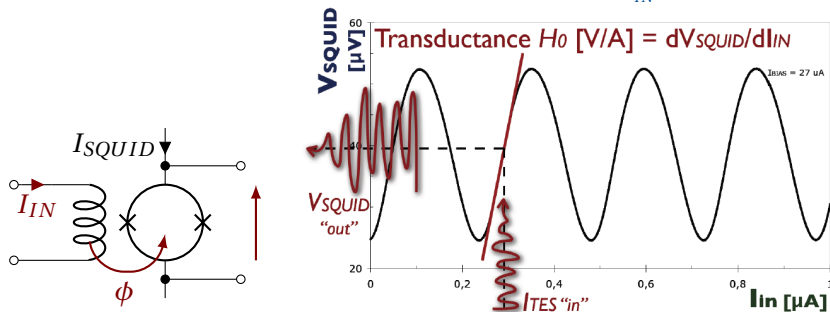
I(V) and $V(\phi)$ characteristic SQUID (Magnetometer)

- ▶ Bias $< 2I_0$: no voltage
- ▶ Bias $> 2I_0$: SQUID has periodic (ϕ_0) characteristic $V(\phi)$



SQUID as a trans-impedance amplifier

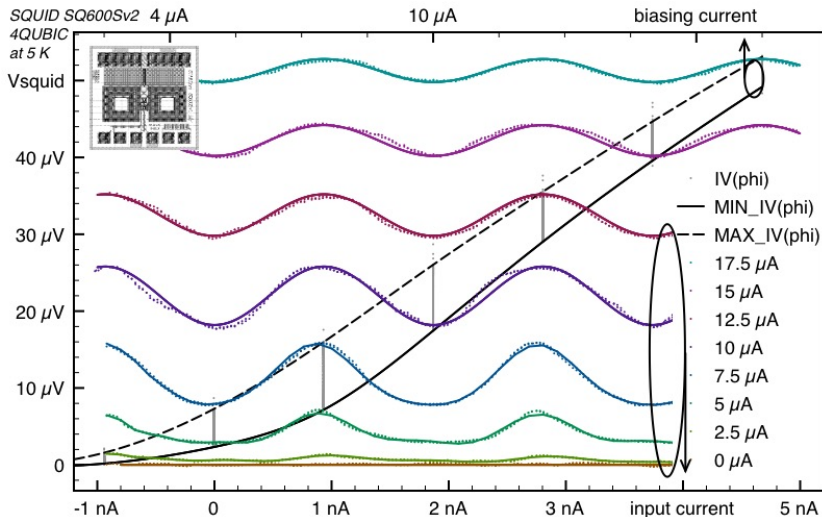
An input loop is used to convert I_{IN} in flux $\phi = \frac{I_{IN}}{M_{IN}}$:



- ▶ Input impedance = 0Ω
- ▶ Input noise $\approx \text{pA}/\sqrt{\text{Hz}}$
- ▶ Trans-impedance gain $\approx 100 \text{ V/A}$

I(V) and V(ϕ) overplot

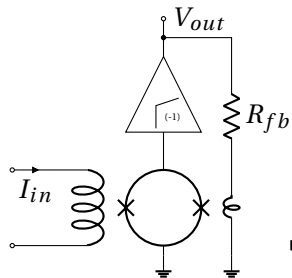
The use of V(ϕ) to measure I(V)



A flux feedback to linearize the SQUID characteristic

An other loop is usually used to compensate magnetic flux induced by I_{in} .

Flux Locked Loop

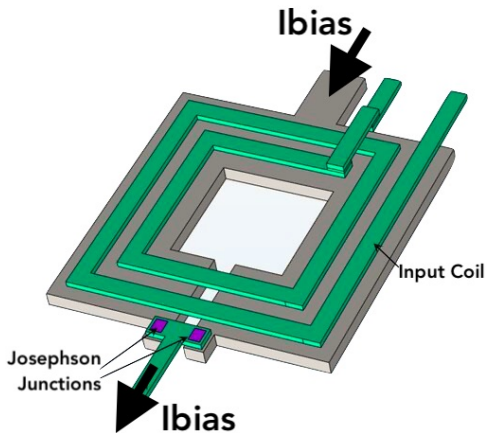


$$|H_{open}| = \left. \frac{V_{out}}{I_{in}} \right|_{open} = H_{0_{SQUID}} G_{Amp}.$$

$$|H_{FLL}| = \left. \frac{V_{out}}{I_{in}} \right|_{close} = \boxed{\frac{M_{in}}{M_{fb}} R_{fb}}$$

☞ Don't worry about the loop gain sign, H_0 is periodic !

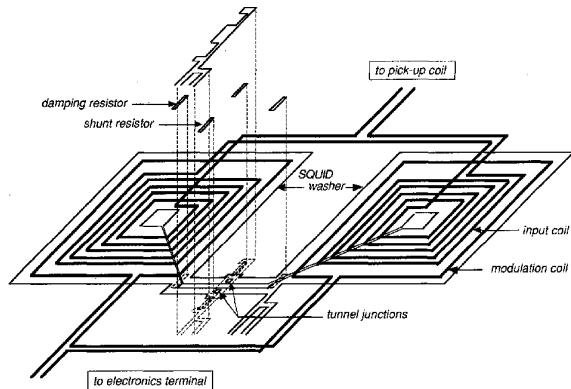
SQUID planar technology



J. S. Bennett et al., Precision Magnetometers for Aerospace Applications: A Review - 2021

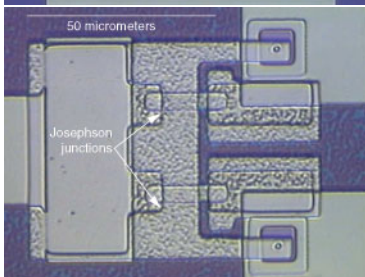
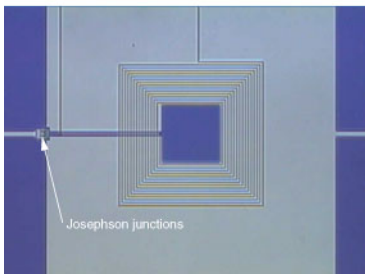
SQUID gradiometry to remove far field magnetic noise

Pickup consists of 2 integrated rectangular coils connected in series and magnetically coupled to a dc-SQUID in a double parallel washer configuration via two crossed multiturn input coils

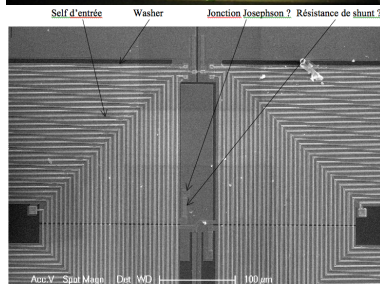
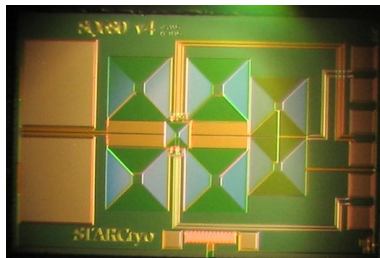


Design and fabrication of multichannel DC SQUIDs for biomagnetic applications S. Yamasaki

Planar technology and gradiometry



Lawrence Livermore National Laboratory



MEB-1ef, SQUID StarCryo

SQUID Noise

- ▶ **Junction flicker noise** : $S_V = (\frac{dI_c}{dT})^2 (\frac{dV}{dI_c})_I^2 k_B T^2 / (3C_V f)$
-> C_V the junction heat capacity -> \forall SQUID geometry
random trapping and release of electrons in the junction barrier, which locally decrease the conductivity and cause the *critical current fluctuation*
- ▶ **Excess 1/f noise** observed two orders of magnitude higher
- ▶ **Shunt Johnson noise** : $S_V = 4k_B T R_{\text{shunt}}$

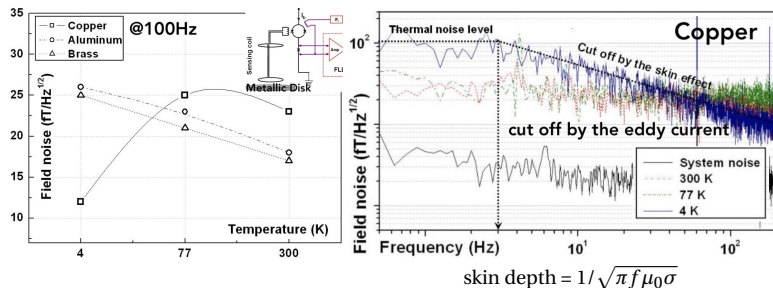
J. Clarke and G. Hawkins, Flicker 1/f noise in Josephson tunnel junctions, Phys. Rev. B 14, 2826 1976

Magnetic Johnson induced noise from normal metal

Thermal motion of charge carriers in a conducting object causes magnetic field noise

can interfere with sensitive detectors : $\sqrt{S_I} = (4k_b T \mu_0^2 / L_0^2 \rho_n) G \propto \sqrt{\sigma} \rightarrow$ increase with cooling

$$\text{with } G = \pi h a^4 / 32 z_0^2$$



K. Yu et al. Direct Measurement of Thermal Noise and Eddy-current Noise Induced in Metals by Using a 1st-order SQUID Gradiometer

J. Clem et al. Johnson noise from normal metal near a superconducting SQUID IEEE 1987

Conclusion

- + Decreasing temperature leads to **reduces the thermal noise**
- ▶ However, **shot noise and flicker noise are not directly improved** with cooling
- Many examples show **significant increase of $1/f$ noise at cryogenic temperatures**

Also : transistor transconductance normalized to a given biasing current is increasing with cooling

However, to reduces the electronic dissipation at cryogenic temperature -> **biasing is also reduce leading to not benefiting larger gain at cryo T**